UNIVERSITÀ DEGLI STUDI DI PADOVA
Department of Land, Environment Agriculture and Forestry

Second Cycle Degree (MSc)
in Food and Health

Targeted prevention of skeletal muscle wasting in cancer cachexia with combinatorial RNAi-based approaches

Supervisor
Prof. Marco Sandri
Co-supervisor
Dott.ssa Roberta Sartori

Submitted by
Asude Berber
Student n. 2040358

ACADEMIC YEAR: 2023/2024

Index

1. Abstract

Cancer cachexia is a wasting syndrome responsible for systemic multi-factorial metabolic dysfunctions leading to severe body weight loss due to excessive muscle and adipose tissue catabolism. The occurrence of cancer cachexia worsens the quality of patients' lives, reduces the efficacy and tolerance to anti-cancer treatments, and most importantly is directly responsible for up to 30% of cancer-related deaths. Currently, no substantial treatments exist for cancer cachexia, and nutritional support does not completely reverse the condition as well.

Skeletal muscle wasting and strength loss are considered among the most deleterious clinical features underlying cancer cachexia and predictors of poor outcomes. Indeed, since in the preclinical models, the preservation of skeletal muscle mass is beneficial for survival, independent of tumor growth, it is crucial to uncover signaling pathways underlying muscle atrophy, in order to identify molecular targets that can potentially counteract muscle loss and cachexia onset. Muscle atrophy arises when hyperactivation of proteolysis and organelle degradation exceeds rates of protein synthesis and organelle biogenesis and involves the transcription of genes encoding for rate-limiting enzymes of the degradative systems. Different pathways control the balance of anabolism and catabolism; among all, the most important ones are Akt/FoxOs, IKK-NF-κB, IL6-JAK-Stat3, and the TGF-β/Myostatin-Smad2/3 pathways. In our study, we focused on the activity of FoxOs, a family of transcriptional factors downstream the IGF1/insulin-Akt pathway whose activity controls the expression of crucial genes belonging to both the autophagy/lysosome system and the ubiquitin-proteasome system including Atrogin1/Fbxo32 and MuRF1/Trim63, two E3-ubiquitin ligases strongly upregulated in different catabolic conditions (including cancer cachexia). They are considered master genes of muscle atrophy, and they are responsible for myofibrillar protein degradation.

In our study, we aim at establishing RNA-based therapeutics methods to prevent muscle wasting and setting up a Spatial Transcriptomics method in muscles to discover underlying gene profiles in tumor-induced muscle loss conditions.

Specifically, our goals are:

i) to generate and validate shRNA constructs against MuRF1 and FoxO1/3 *in vitro*;

ii) to perform *in vivo* muscle delivery and validation of shRNA oligos against MuRF1 and FoxO1/3 alone or in combination in the context of cancer-mediated muscle atrophy;

iii) to set up a spatial transcriptomic approach in control and cachectic muscles transfected with shRNA oligos against MuRF1 and FoxO1/3 with the final goal of studying and comparing the transcriptome between these three experimental groups.

Our preliminary results show that knocking down of FoxO1/3 and MuRF1 alone in tumor-bearing mice induced partial protection of tumor-induced muscle loss, even if it was not sufficient to cause muscle growth in the control group. However, knocking down the combination of both FoxO1/3 and MuRF1 expressions completely protected cancer-induced muscle loss and was sufficient to mediate a hypertrophic effect in the skeletal muscles of the control group.

These results suggest that there might be synergistic roles between FoxO1/3 and MuRF1 activities. The spatial transcriptomic approach will allow us to understand the underlying molecular pathways, and genes profiles activity in the course of cancer cachexia, and the rescue condition of cachectic signature with a combinatorial knockdown approach of FoxO1/3 and MuRF1.

To conclude, our experimental results and potential future goals aim to create novel combinatorial RNAi-based muscle-targeted therapeutic methods to counteract skeletal muscle wasting in cancer cachexia. The discovery of a novel targeted treatment approach could lead to the amelioration of cancer cachectic patients' lives and prevent cancer-induced deaths.

2. Riassunto

La cachessia da cancro è una sindrome da deperimento responsabile di disfunzioni metaboliche sistemiche multifattoriali che portano a una grave perdita di peso corporeo dovuta a un eccessivo catabolismo del tessuto muscolare e adiposo. La cachessia oncologica peggiora la qualità della vita dei pazienti, riduce l'efficacia e la tolleranza ai trattamenti antitumorali e, soprattutto, è direttamente responsabile fino al 30% dei decessi correlati al cancro. Attualmente non esistono trattamenti sostanziali per la cachessia da cancro, e anche il supporto nutrizionale non inverte completamente la condizione.

Il deperimento dei muscoli scheletrici e la perdita di forza sono considerati tra le caratteristiche cliniche più deleterie alla base della cachessia da cancro e predittori di esiti sfavorevoli. Infatti, poiché nei modelli preclinici la conservazione della massa muscolare scheletrica è benefica per la sopravvivenza, indipendentemente dalla crescita del tumore, è fondamentale scoprire le vie di segnale alla base dell'atrofia muscolare, al fine di identificare bersagli molecolari che possano potenzialmente contrastare la perdita muscolare e l'insorgenza della cachessia.

L'atrofia muscolare si verifica quando l'iperattivazione della proteolisi e della degradazione degli organelli supera i tassi di sintesi proteica e di biogenesi degli organelli e coinvolge la trascrizione di geni che codificano per gli enzimi chiave coinvolti nei processi degradativi. Diverse vie controllano l'equilibrio tra anabolismo e catabolismo; tra tutte, le più importanti sono Akt/FoxOs, IKK-NF-κB, IL6-JAK-Stat3 e le vie TGF-β/Miostatina-Smad2/3. Nel nostro studio, ci siamo concentrati sull'attività di FoxOs, una famiglia di fattori trascrizionali a valle della via IGF1/insulina-Akt, la cui attività controlla l'espressione di geni cruciali appartenenti sia al sistema autofagico/lisosomioale sia al sistema ubiquitina-proteasoma, tra cui Atrogin1/Fbxo32 e MuRF1/Trim63, due E3-ubiquitina ligasi fortemente upregolate in diverse condizioni cataboliche (compresa la cachessia da cancro). Esse sono considerate due geni master dell'atrofia muscolare e sono responsabili della degradazione delle proteine miofibrillari.

Nel nostro studio, ci proponiamo di stabilire metodi terapeutici basati sull'RNA per prevenire il deperimento muscolare e di mettere a punto un protocollo di trascrittomica spaziale nei muscoli per scoprire i profili genici sottostanti la condizione di perdita muscolare indotta da tumori.

In particolare, i nostri obiettivi sono:
i) generare e validare costrutti shRNA contro MuRF1 e FoxO1/3 in vitro;
ii) eseguire la somministrazione in vivo di oligo shRNA contro MuRF1 e FoxO1/3 da soli o in combinazione nel contesto dell'atrofia muscolare mediata dal cancro;
iii) mettere a punto un approccio di trascrittomica spaziale in muscoli di controllo, cachettici e cachettici trasfettati con oligo shRNA contro MuRF1 e FoxO1/3, con l'obiettivo finale di studiare e confrontare il trascrittoma tra questi tre gruppi sperimentali.

I nostri risultati preliminari mostrano che l'abbattimento singolo di FoxO1/3 o MuRF1 in muscoli di topi portatori di tumore ha indotto una parziale protezione della perdita muscolare indotta dal tumore, anche se non è stato sufficiente a causare una crescita muscolare nel gruppo di controllo. Tuttavia, l'abbattimento combinato dell'espressione di FoxO1/3 e MuRF1 ha protetto completamente la perdita muscolare indotta dal tumore ed è stato sufficiente a mediare un effetto ipertrofico nei muscoli scheletrici del gruppo di controllo.

Questi risultati suggeriscono che potrebbero esserci ruoli sinergici tra le attività di FoxO1/3 e MuRF1. L'approccio trascrittomico spaziale ci permetterà di comprendere le vie molecolari sottostanti e il profilo di espressione genica nel corso della cachessia tumorale e di studiare come il trascrittoma del muscolo cachettico venga modificato/revertito dall'approccio combinatorio di knockdown di FoxO1/3 e MuRF1.

In conclusione, i nostri risultati sperimentali e i potenziali obiettivi futuri mirano a creare nuovi metodi terapeutici combinati basati su RNAi mirati al muscolo per contrastare il deperimento del muscolo scheletrico nella cachessia da cancro. La scoperta di un nuovo approccio terapeutico mirato potrebbe migliorare la vita dei pazienti cachettici e prevenire i decessi indotti dal cancro.

3. Acknowledgments

In the completion of this thesis, I would like to take this opportunity to express my appreciation who enlightened, trained, and helped me to expand my knowledge and skills in this journey.

First of all, I would like to present special thanks to Marco Sandri, who gave me this opportunity to conduct my thesis and acquaint me in every meeting with his extensive knowledge.

With my deepest appreciation, I am extremely grateful to Roberta Sartori, who mentored me and gave an insight into every experiment with her expertise. I am and will be always thankful for her endless support and contribution to my research journey.

I would like to extend my sincere thanks, but words cannot be enough to express my gratitude to Camilla Pezzini, who trained me, contributed to improving myself, and taught me everything with her infinite patience. I could have not undertaken this journey without her support, and I will never forget what she taught me and how much she contributed to my expanding scientific fund of knowledge.

I also would like to thank my family and friends who always support me persistently in everything that I pursue. I am thankful to them for opening my horizons, to giving me every opportunity that I would like to have.

Finally, my gratitude also goes to all lab members for creating a supportive research environment, and for always being helpful.

4. Introduction

4.1. Skeletal muscle

Skeletal muscle is the most occupant tissue in the human body, responsible for almost ~50% of whole-body protein turnover, and it consists of water (mainly), protein, carbohydrates, fat, minerals, and inorganic salts. (Frontera & Ochala, 2015). Skeletal muscle plays a sustainable role in metabolic programming, including the regulation of glucose, lipids and amino acids metabolism and homeostasis. Moreover, total muscle mass homeostasis depends on the equilibrium between anabolic (protein synthesis) and catabolic (protein degradation) processes, which are sensitive to hormonal and nutritional status, physical activity, injury, and diseases (e.g. cancer, diabetes) (Sartori, Romanello, et al., 2021a). Whenever this equilibrium is perturbed, for instance when protein degradation is highly induced, muscle loss may occur, being a poor prognostic indicator that can impair the efficacy of several therapeutic treatments (Frontera & Ochala, 2015).

4.1.1. Skeletal muscle structure and its function

Skeletal muscle is a striated, innervated, highly vascularized, and organized tissue that contains several bundles of muscle fibers (myofibers) that represent a muscle cell. Each muscle fiber is surrounded by a plasma membrane called the sarcolemma, (Frontera & Ochala, 2015; Gillies & Lieber, 2011). Groups of parallel disposed myofibers are organized in bundles termed fascicles, and surrounded by a thick layer of connective tissue, the perimysium.

A dense connective tissue layer, the epimysium, encapsulates the entire muscle and identifies its volume. (Mukund & Subramaniam, 2020a). The epimysium thickens and merges with tendons, specialized structures mainly composed by extracellular matrix (ECM), that ensure a functional link between the skeletal muscles and the bone (Kjær, 2004).

Within skeletal muscle tissue, blood vessels and nerves travel through the epimysium, perimysium and endomysium branching into the muscle and reaching the individual muscle fibers.
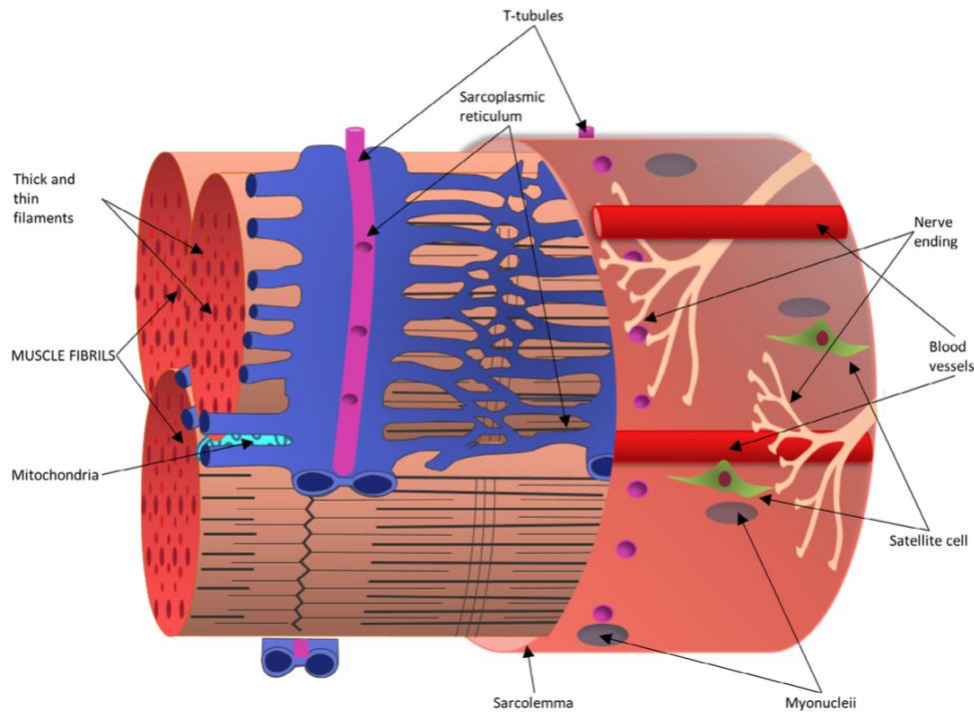
Figure 1: Schematic representation of muscle fiber (Mukund & Subramaniam, 2020a)

Skeletal muscle is called striated muscle because of the organization of a rearranged series of contractile filaments which are known as sarcomeres, that are the functional unit of the muscle (Sweeney & Hammers, 2018).

Contraction of the sarcomere allows striated muscle function force generation and rapid movement. Sarcomeres, which compose the complex structure, are formed by myosin (thick filaments), and a-actin (thin filaments) with their associated proteins. Furthermore, the sarcomere is distinguished by distinct regions which are divided by the Z-disk at each end with a narrow dark line. Each Z-disk is positioned in the middle of a lighter I band that is commonly shared between neighboring sarcomeres. In the center of the sarcomere lies the dense A-band,

primarily composed of thick filaments, accompanying a lighter H-zone at its center. The M-line halves this H-zone. Thin filaments are assembled laterally at the Z-disk, while the M-band serves as a structural link connecting the thick filaments (Mukund & Subramaniam, 2020a).
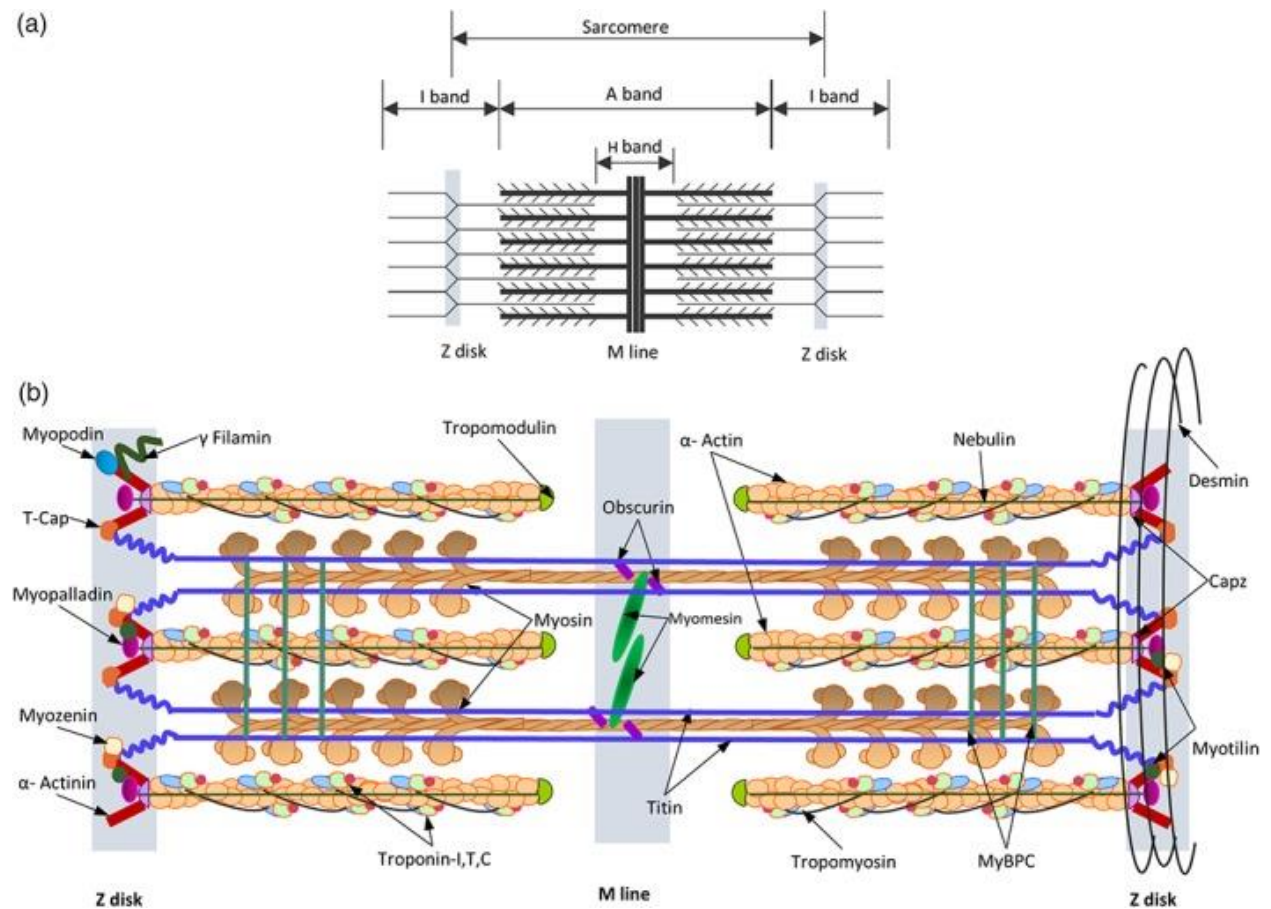
Figure 2: (a) It represents the scheme of the striated skeletal muscle sarcomere with the coordination of thick and thin filaments in the sarcomere and designating bands of overlap between them. **(b)** Schematic representation of the location of major sarcomeric proteins and their organization (Mukund & Subramaniam, 2020a).

In the broader context of muscle function, it is recognized fact that muscle fibers' size directly correlates with their ability to generate force, and muscle fibers maintain a uniform diameter independent of the muscle's overall size (Mukund & Subramaniam, 2020a).

Regarding muscle functionality, muscle contraction specifically starts with the binding of troponin-C to the calcium ions (Ca^{2+}) released during Excitation-Contraction Coupling (ECC). This interaction induces a change in the troponin-tropomyosin complex by exposing myosin-binding sites on the actin filaments. Afterwards, myosin heads attach to these sites and proceed along the length of the actin filament, which subsequently involves ATP hydrolysis and culminates in muscle contraction with the conclusion of generating force within each myofibril (Sweeney & Hammers, 2018).

4.1.2. Skeletal muscle fiber types

The adaptability of muscles to perform a wide range of functions, such as maintaining posture, executing repeated moderate contractions, and generating rapid and powerful maximal contractions, relies on the presence of various types of muscle fibers within each muscle, since each fiber type possesses unique characteristics like contraction speed, maximum power output, ability to shorten quickly, and fatigue resistance (Bottinelli & Reggiani, 2000).

Skeletal muscle fiber types are constituted by four types of muscle fibers upon two main types; slow-twitch (Type I) and fast-twitch (Type II) fibers containing subtypes IIA, IIB, and IIX.
Focusing on the main ones, slow-twitch muscles are known for their high vascularization, abundant mitochondria, and myoglobin content; they are characterized by a strong oxidative metabolism and low glycolytic activity. These fibers are resistant to fatigue and predominate in prolonged contractions with relatively low force (found in elite endurance athletes like swimmers). On the other hand, fast-twitch muscles contract quickly but fatigue quickly. They hinge on glycolysis for energy production and are prevalent in elite strength and power athletes such as sprinters and weightlifters (Bottinelli & Reggiani, 2000; Mukund & Subramaniam, 2020a).

4.2. Plasticity of Skeletal Muscle and Muscle Atrophy

Skeletal muscle has great plasticity to adapt to stimuli such as exercise, denervation, nutritional interventions, and environmental factors (i.e. hypoxia) (Flück & Hoppeler, 2003). In response to external stimuli, any alteration in skeletal muscle mass affects the functional performance and regenerative capacity of the tissue itself (Scicchitano et al., 2018).

When protein degradation exceeds protein synthesis, muscle atrophy takes place, causing a reduction in the cross-sectional area of myofibers and a decreased muscle strength. Since skeletal muscle plays a key role in whole-body metabolism, perturbations in this tissue have a vital role in the health, survival, and adaptability of organisms. Therefore, diseases and conditions that lead to an induction of protein catabolism such as sepsis, cancer, burns, diabetes, starvation, organ failure, and infections result in muscle wasting (muscle atrophy), which also exacerbate conditions of diseases with different physiological and pathological causes (Fanzani et al., 2012; Vainshtein & Sandri, 2020). For instance, in cancer cachexia, skeletal muscle wasting represents a major cause of total body wasting in cancer patients, and it highly negatively contributes to anti-cancer treatment, increasing the mortality of cancer patients (Schmidt et al., 2018a).

4.2.1. Protein degradation systems

Muscle atrophy is characterized by a decrease in cell size with the loss of proteins, organelles, and cytoplasm. Induced Degradation system occurring in muscle loss contributes to an impairment in cellular turnover and a decrease in protein turnover (Sandri, 2008).

Atrophic skeletal muscle shares common pathways and transcriptional regulators that coordinates the activation of genes responsible for atrophic conditions.

Particularly, among protein degradation signaling pathways, ubiquitin–proteasome and autophagy–lysosome systems are the major ones controlling protein turnover in skeletal muscle.(Sartori, Romanello, et al., 2021a).
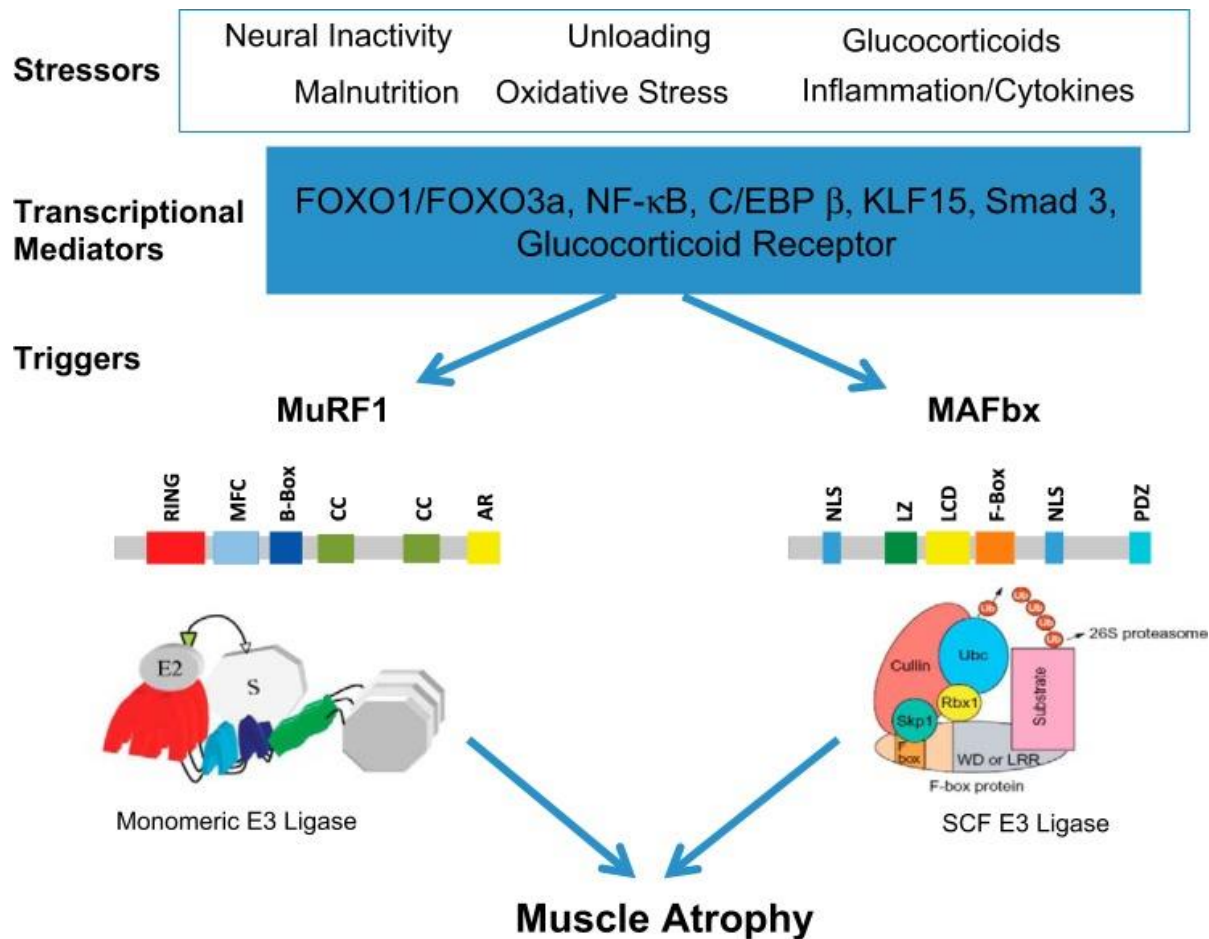
Figure 3: Schematic representation of how stressors and transcriptional mediators regulate muscle RING finger 1 (MuRF1) and muscle atrophy F-box (MAFbx) proteins' expressions in skeletal muscle, and their domain structures. Stressors induce skeletal muscle atrophy, as illustrated. These trigger the induction of expression of transcription factors which include the forkhead transcription factors (FOXO1 and FOX03a), NF-κB transcription factors (p65, c-Rel, RelB, p52, and p50), CCAAT/enhancer-binding protein-β (C/EBPβ), kruppel-like factor-15 (KLF-15), and/or activation of the glucocorticoid receptor. These induced transcriptional factors bind to the promoter regions of either the MuRF1 or MAFbx genes leading to an increase in their expression levels within the muscle.

As their default domain structures, MuRF1 covers a RING finger domain (RING), a MuRF1 family conserved domain (MFC), a B-box domain (B-Box), coiled-coil domains (CC), and an acidic tail region (AR). MAFbx covers 2 nuclear localization signals (NLS), a leucine-zipper domain (LZ), a

leucine-charged residue-rich domain (LCD), an F-box domain (F-box), and a PDZ domain (PDZ). SCF, Skp1-Cullin1-F-box protein (Bodine & Baehr, 2014a).

4.2.2. Ubiquitin-proteasome system

Various muscle-wasting conditions increase muscle proteolysis which occurs due to the ATP-dependent ubiquitin-proteasome pathway (Bodine & Baehr, 2014a).

Ubiquitinated proteins are degraded into small peptides and free amino acids that can be reused for synthesis of new proteins or for energy production.

E1 (ubiquitin activating), E2 (ubiquitin conjugating) and E3 (ubiquitin ligase) are classes of enzymes that are involved in protein ubiquitination that cooperate in the primary polyubiquitination step in a series of catalytic reactions.

It is known that several ubiquitin ligases (E3) have delineated roles in muscle contributing to maintain protein turnover and guarantee correct homeostasis (Sacheck et al., 2007) In consequence of catabolic condition there is an enhanced expression of transcripts encoding E3 ligases (Bonaldo & Sandri, 2013).

MuRF1 (Trim63) and F-box protein atrogin-1/MAFbx are the first muscle-specific E3 ubiquitin ligases identified. highly induced expression of these two ubiquitin ligases has been observed in atrophic (Bodine & Baehr, 2014a; Lecker et al., 2006). MuRF1 tends to ubiquitinate muscle structural proteins such as troponin I, myosin heavy chains, actin, myosin-binding protein C and myosin light chain 1 and 2. Atrogin-1 targets substrates that are related to the growth-related mechanisms or survival pathways. Moreover, MAFbx (or atrogin-1) protein contains E3 ubiquitin ligases motif, and it is a cardiac- and skeletal muscle-specific F-box protein that binds to Skp1, Cul1, and Roc1 which are constituents of SCF ubiquitin ligase complexes. It has been found that the MAFbx has a function in preventing pathologic hypertrophy by binding to calcineurin, which is targeted by K48-linked ubiquitin chains, and promoting its ubiquitylation and proteasome-

dependent degradation (Li et al., 2007). Nevertheless, knockout animals lacking either MuRF1 or Atrogin-1 are partially protected from muscle loss in catabolic conditions such as denervation or sarcopenia. These observations may suggest that additional E3s contribute to muscle loss.

4.2.3. Autophagy–lysosome system

The autophagy-lysosomal system is a conserved catabolic system, essential for metabolic homeostasis maintenance. It's responsible for the degradation of cytosolic components by removing misfolded or aggregated proteins, clearing damaged organelles, as well as eliminating intracellular pathogens during physiological and catabolic conditions.

Autophagy, also referred to as macroautophagy, consists in the formation of a pre-autophagosomal structure, a double membrane-bound vesicle called the autophagosome that engulfs the cargo that needs to be degraded. This lysosomal macroautophagy system is one of the major proteolytic pathways induced in response to starvation or catabolic conditions (Bechet et al., 2005).

In terms of energy homeostasis and macromolecule turnover processes in skeletal muscle, the autophagic pathway plays a key role. Aberrant autophagy in muscles leads to mitochondrial damage, endoplasmic reticulum stress, disrupted sarcomeric-protein turnover, and cell death (Bonaldo & Sandri, 2013). Excessive autophagy activity occurs in pathologic conditions such as cancer cachexia, fasting, sepsis, critical illness, cirrhosis, chemotherapy, disuse, denervation due to ongoing stress, cell metabolite generation, and removal of damaged components Autophagy shows some selectivity in terms of mitophagy or protein aggregates (Sartori, Romanello, et al., 2021a). For instance, the proteins parkin, PINK1, Bnip3, and Bnip3L have role in regulation of mitophagy, and inactivation of these genes results in mitochondrial abnormalities (Sandri, 2013). Indeed, mitochondrial abnormalities, such as altered expression of the fission machinery and dysfunctional mitochondria, are observed in atrophying muscles by active muscle loss or myofiber degeneration (Romanello & Sandri, 2010). The genes coding for autophagy-related proteins;Atg7, Atg5, NAF-1 (nutrient-deprivation autophagy factor), VPS15, ULK2, AMPK and mTOR (Raun, Ali, et al., 2022; Raun, Knudsen, et al., 2022) have been observed having an

altered gene expression in murine model of cancer cachexia resulting in metabolic dysfunction (Masiero et al., 2009; Sandri, 2013; Sartori et al., 2021). The findings make an important conclusion on the linkage between the autophagy-lysosome system and cancer cachexia. This is because the altered lysosomal activity has been already reported as one of the main features occurring in many muscle catabolic conditions. Indeed autophagy-related genes have been indicated to be upregulated in muscle in denervation or in fasting condition via a FoxO3-dependent mechanism (Penna et al., 2013).

Moreover, in previous research, it has been found that FoxO transcription factors and active expression of FoxO3 play a key role in muscle fiber atrophy and activation of atrogin-1/MAFbx atrophic markers on the occasion of denervation, fasting, and glucocorticoid treatment (Sandri et al., 2004).

According to past research, in the autophagy-lysosomal system, FoxO3 has an important effect in the stimulation of lysosomal proteolysis by activating autophagy via decreased IGF-1-PI3K-Akt signaling activity, which is an important hypertrophic signaling pathway (Zhao et al., 2007).

4.3. Muscle hypertrophy

Skeletal muscle hypertrophy consists in an increase in protein synthesis and a decrease in protein degradation, resulting in the accumulation of proteins and increasing fiber area. The mechanism at work involves muscles generating force in response to resistance exercise. Additionally, this process triggers the release of growth factors and activates signaling pathways (Miyazaki & Esser, 2009).

4.3.1. Insulin/IGF1-Akt-mTOR signaling pathway

The signaling pathway of IGF1-Akt-mTOR (growth factors like Insulin-1, phosphatidylinositol 3-kinase, and protein kinase B) is one of the main mediator pathways involved in the development of muscle mass and underlying muscle hypertrophy (Fernandes et al., 2012).

Insulin-like growth factor-1 (IGF-1) is one of the best-recognized growth factors, and it has a key role in modulating muscle size regulating muscle function and promoting growth relative to the outcomes of physical activity as well.
At the molecular level, when IGF-1 receptor (IGF-1R) binds to IGF-1 and phosphorylates an intracellular adaptor protein insulin receptor substrate-1 (IRS-1), induces the recruitment of phosphoinositide 3-kinase (PI3K) as well as Akt phosphorylation (Yoshida & Delafontaine, 2020).

The Akt protein family, which is composed of Akt1 and Akt2 isoforms, whose isoforms are specifically expressed in skeletal muscle. Those isoforms are triggered by activation/phosphorylation of growth factors, cytokines, and hormones, which takes place by relying on PI3K (phosphatidylinositol 3 kinase) (Fernandes et al., 2012). Moreover, in one of the recent studies, it has been shown that deletion of two isoforms of Akt (Akt-1 and Akt-2) ended in muscle atrophy (Jaiswal et al., 2019).

mTOR, a mammalian target of rapamycin, is one of the major players in controlling skeletal muscle mass in the context of hypertrophy. mTORC1 and mTORC2 constitute catalytic subunits of mTOR (Yoon, 2017).

It had been found that mTORC1 signaling was weakened in the Lewis lung carcinoma (LLC) and in Colon-26 (C26) tumor-bearing mice with protein synthesis reduction effect, moreover, activation of Akt-mTORC1 signaling retrieved muscle mass loss and force by 15-20% (Geremia et al., 2022).

In addition to mTOR, IGF-1/Akt is known to be controlled by another protein signaling pathway via glycogen synthase kinase 3β (GSK3β). The Akt-mediated phosphorylation of GSK3β constitutes another crucial downstream pathway influenced by IGF-1. In conditions promoting muscle hypertrophy, GSK3β undergoes phosphorylation, effectively inhibiting its activity. This leads to activation of eIF2B and the transcriptional activator β-catenin. It has been observed that GSK3β activity is increased in muscle atrophy induced by dexamethasone (Dex). Distinctively, IGF-1 or constitutively active Akt gene transfer has been shown to inhibit GSK3β, elevate β-catenin levels, and effectively prevent muscle atrophy (Yoshida & Delafontaine, 2020).
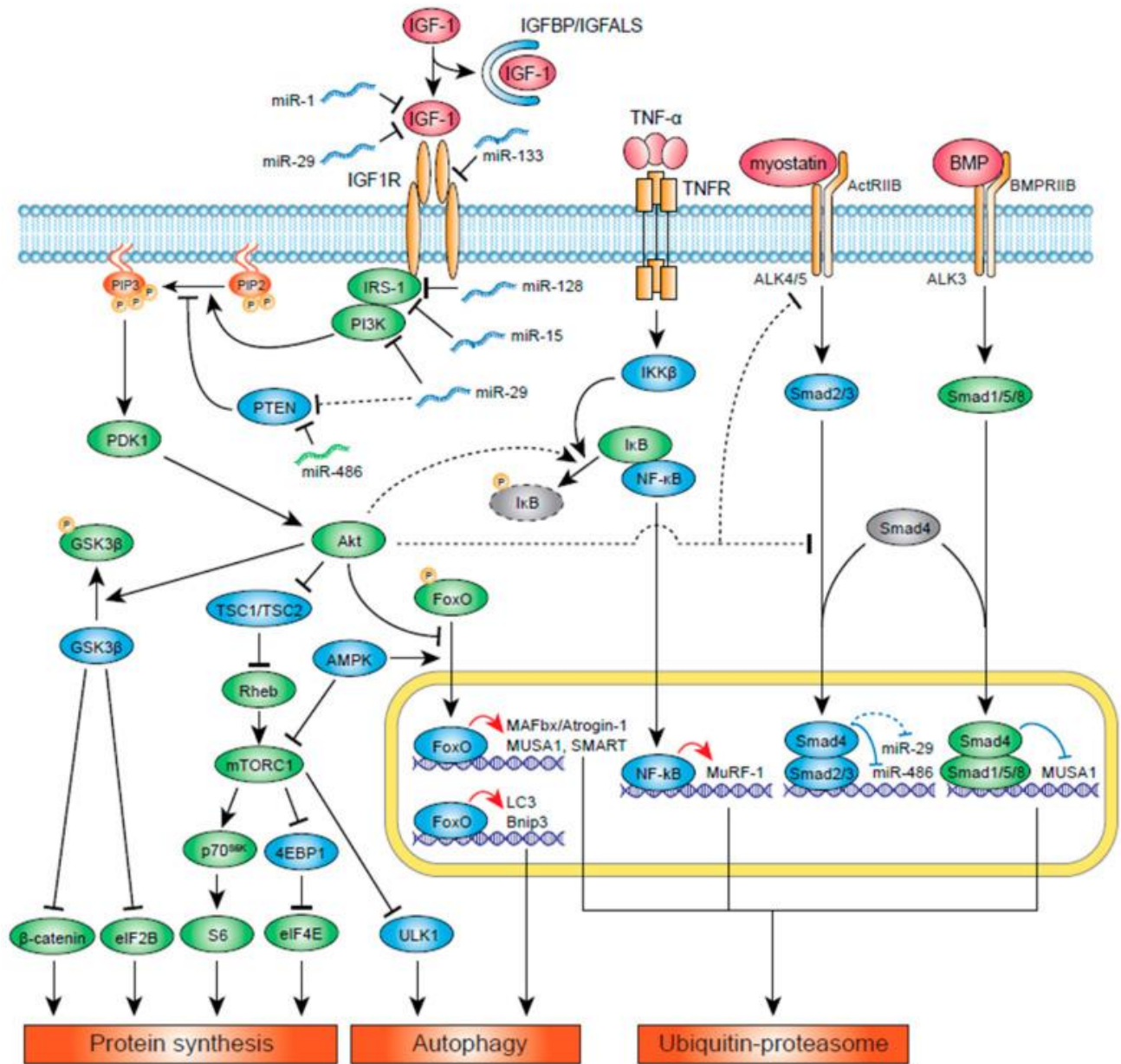
Figure 4: The representation scheme of signaling molecules that induce and/or inhibit protein synthesis and protein degradation. The molecules that induce protein synthesis are illustrated in green, on the contrary, the blue ones illustrate the molecules that inhibit protein synthesis by activating protein degradation. The insulin-like growth factor 1 (IGF-1) is bound to IGFBP and IGFALS, this suppresses the activity of IGF-1. Once IGF-1 binds its receptor IGF-1R, it recruits the activation of IRS-1 and PI3K. PI3K transforms PIP2 into PIP3, leading to the activation of PDK1 and

Akt. Akt, in turn, triggers protein synthesis by activating ribosomal protein S6 and translation initiation factor eIF4E through mTORC1. Additionally, Akt activates β-catenin and eIF2B downstream of GSK3β. Akt can inhibit ubiquitin-proteasome system (UPS) activity via inhibition of FoxO-mediated transcription of E3 ubiquitin ligases MAFbx/Atrogin-1, MUSA1, and SMART. Even though FoxO-mediated transcription factors induce the expression of MuRF1 (Wilburn et al., 2021), the expression of MuRF1 is also induced by cytokines such as TNF-α via the NF-kB pathway. Moreover, myostatin and BMP signaling players compete for the recruitment of Smad4. Activation of myostatin downregulates BMP-mediated Smad1/5/8 activation, resulting in the inhibition of MUSA1-mediated UPS activity. Akt may have a role also in the downregulation of ActRIIB and inhibition of ALK4/5. The underlying mechanism is currently unknown as illustrated in dotted lines.

As illustrated here, several miRNAs also play a key role in the activation and/or degradation of protein synthesis (Yoshida & Delafontaine, 2020).

4.4. Cancer-associated cachexia and metabolism

Cachexia is a metabolic disorder that can be defined as unintentional body weight loss and disrupted homeostatic system of the body in terms of both energy and protein balance in the presence of a tumor (Baracos et al., 2018). It is well known that cancer-related cachexia diminishes the efficacy of cancer treatment by increasing the toxicity of chemotherapy, thereby resulting in decreased quality of life and increased mortality ratio of cancer patients. All these reasons make cachexia a multifactorial metabolic syndrome as a result of elevated catabolism and inflammation with significant loss of skeletal muscle mass (with or without loss of fat mass) that cannot be rescued by nutritional support (Baracos et al., 2018; Schmidt et al., 2018a).

The determined diagnostic criterion for cachexia is involuntary weight loss of more than 5% in the last 6 months, weight loss of more than 2% in individuals with lower than 20 kg/m^2 body-mass index (BMI), or weight loss of more than 2% in the individuals with low muscularity such as sarcopenic individuals (K. Fearon et al., 2011).

Cancer cachexia is constituted of three clinical stages: pre-cachexia, cachexia, and refractory cachexia, yet patients might not experience all three stages consecutively as well as the incidence and the level of cachexia rely on type, location, and stage of the tumor (Ni & Zhang, 2020a). Even though there is no current clinical stage identification on pre-cachexia, the SCRINIO Working Group proposed a definition as less than 10% weight loss for pre-cachectic stage; more than 10% weight loss for cachectic stage (Bozzetti & Mariani, 2009).
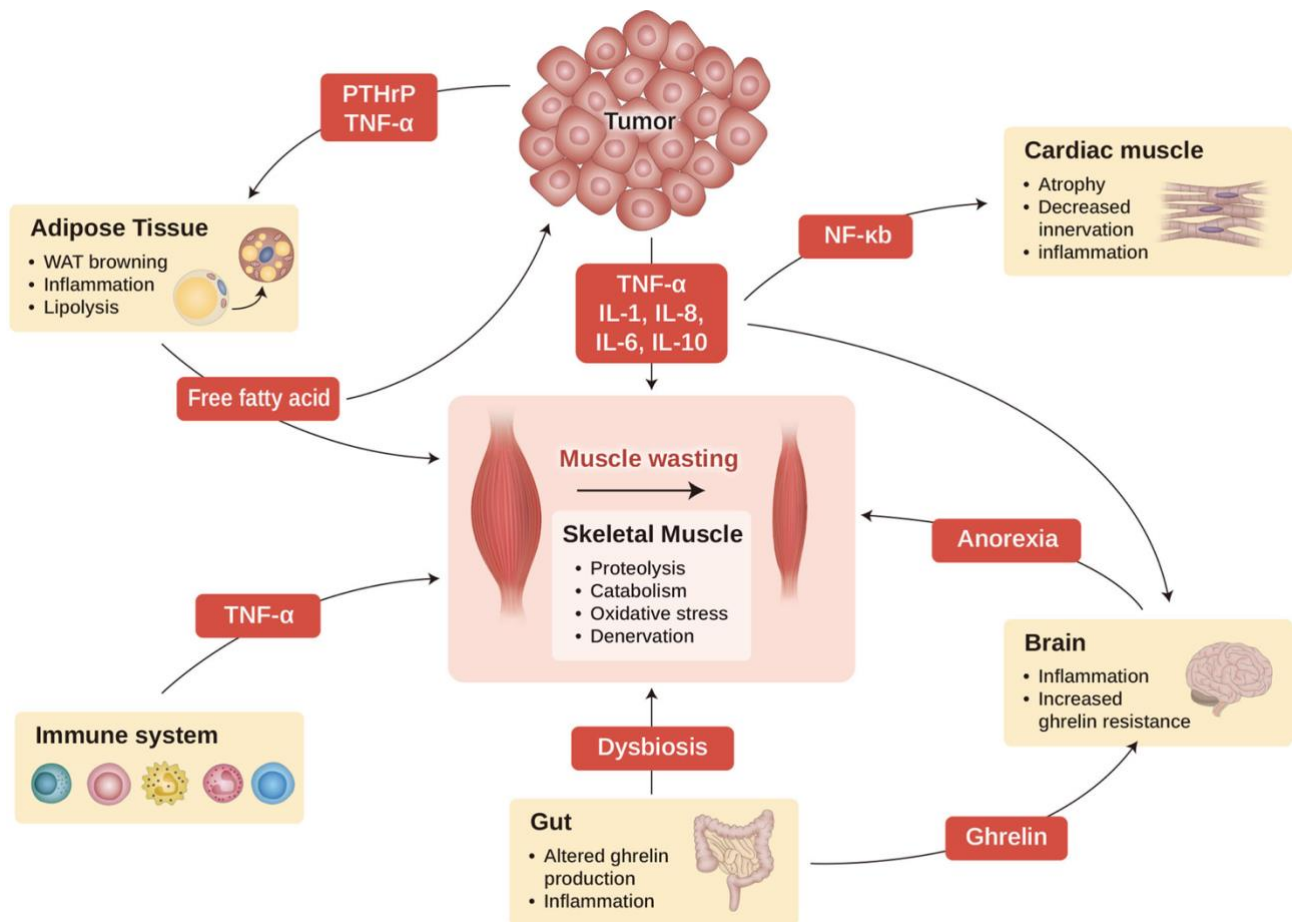
Figure 5: The illustration of cancer cachexia as a multi-organ syndrome (Setiawan et al., 2023). As a result of cachexia, major organs are affected in different ways. Mainly, cancer cachexia affects skeletal muscle and is dependent on the interaction with other organs, such as adipose tissue, brain, gut, cardiac muscle, and immune cells. Cachexia-inducing tumor cytokines also have a role in muscle wasting as well as interaction with other organs (brain, cardiac muscle, gut, and adipocyte tissue), which worsens cachexia syndrome. WAT, white adipocyte tissue; PTHrP, parathyroid hormone-related protein; TNF-α, tumor necrosis factor-α; IL-1, interleukin-1; IL-6, interleukin 6; IL-8, interleukin-8; IL-10, interleukin 10; and NF-kB, nuclear factor kappa-light-chain-enhancer of activated B cells.

4.4.1. Skeletal muscle wasting in cancer cachexia

Muscle atrophy is one of the key features of cancer cachexia regardless of body mass index (BMI) that has been associated with physical immobility, fatigue, increased risk of respiratory failure, and risk of decreased life span (Aversa et al., 2017).

4.4.2. Cancer cachexia signaling mediators that affect protein homeostasis

Cancer-associated cachexia, as it is already known, is a complex metabolic syndrome that includes systemic induction of pro- and anti-inflammatory cytokines, signaling pathways, and mediators of further hormones, neuropeptides, and tumor-derived factors (Mueller et al., 2016). As a consequence of systemic inflammation, the proteolysis-inducing factor which activates the nuclear factor-kappa B (NF-kB) pathway, expressed by the tumor, induces the production of cytokines and chemokines. This inflammatory situation enables the induction of signal transducer and activator transcription factor 3 (STAT3) pathway as well, which leads to circulating levels of IL-8, IL-6, tissue necrosis factor-alpha (TNF-α), IL-1β, monocyte chemoattractant protein-1 (MCP-1) which leads to the production of myostatin, growth and differentiation factor 15 (GDF-15) and activin-A (Malla et al., 2022).

4.4.2.1. F-BOX proteins in cancer cachexia and muscle wasting

Patients with cachexia encounter impaired muscle homeostasis which results in muscle atrophy supported by continuous activation of the SCF ubiquitin ligase (F-BOX) family member Atrogin-1 (also known as MAFBx/FBXO32) and MuRF1. E3 ubiquitin ligase is a main regulator of muscle wasting via MAFBx/FBXO32/Atrogin-1 which belongs to the F-BOX family (Sukari et al., 2016). it is well established that an induced Atrogin-1 expression leads to muscle mass loss (Bodine et al., 2001a). F-BOX family members, FoxOs transcription factors, are distinguished by a DNA binding domain. This family comprises four members: Foxo1 (FKHR), FoxO3a (FKHRL1), FoxO4 (AFX), and

FoxO6. FoxOs factors play several functions at cellular level, such as controlling the cell cycle, apoptosis, atrophy, DNA repair, managing energy metabolism, and protecting against oxidative stress (Clavel et al., 2010). FoxO transcription factors activity and FoxO cellular localization are affected by the downstream target of the PI3K/Akt signaling pathway (Clavel et al., 2010). It has been found that in atrophic conditions phosphatidylinositol 3-kinase (PI3K)/Akt activity decreases, causing the nuclear translocation of FoxO3a and inducing Atrogin-1 expression in skeletal muscle (Sandri et al., 2004). Moreover, generation of transgenic mice specifically overexpressing FoxO1 in skeletal muscle demonstrated reduced overall skeletal muscle mass in addition to a significant decrease in type I (slow-twitch, low glycolytic) muscle fibers (Kamei et al., 2004). From recent works, the pivotal role of the Forkhead box (FoxO) signaling pathway in cancer cachexia is emerged, since it has been observed its elevated expression in skeletal muscle during cancer cachexia. Blocked FoxO proteins' transcription activity in tibialis anterior (TA) and soleus muscles of tumor-bearing mice indicated decreased levels of Atrogin-1, MuRF1, and Bnip3 expression preventing muscle wasting during cancer cachexia (Reed et al., 2012).

It has been proved that FoxO1 and FoxO3 are influential inducers of MuRF1 expression in atrophic conditions (Peris-Moreno et al., 2020). In vitro study showed that in human and mouse myotubes undergoing serum and amino acid starvation on, FoxO3 promotes an increase in the expression of MuRF1, and Smad3 collaborates with FoxO3 to enhance MuRF1 expression. Smad3 alone had been seen as insufficient to activate MuRF1 transcription and, instead, could be a co-activator (Bollinger et al., 2014). Furthermore, in one study constructed knock-out of FoxOs (FoxO3, FoxO1, and FoxO4) in colon-26 (C26) adenocarcinoma tumor-bearing mice demonstrated that downregulation of other atrophy-related transcription factors (i.e. AP-1, IL-6, C/EBPβ) which plays a critical role in tumor-induced muscle wasting. These findings suggested that FoxOs could have regulator effect on the genes which parted in proteolysis (Judge et al., 2014).
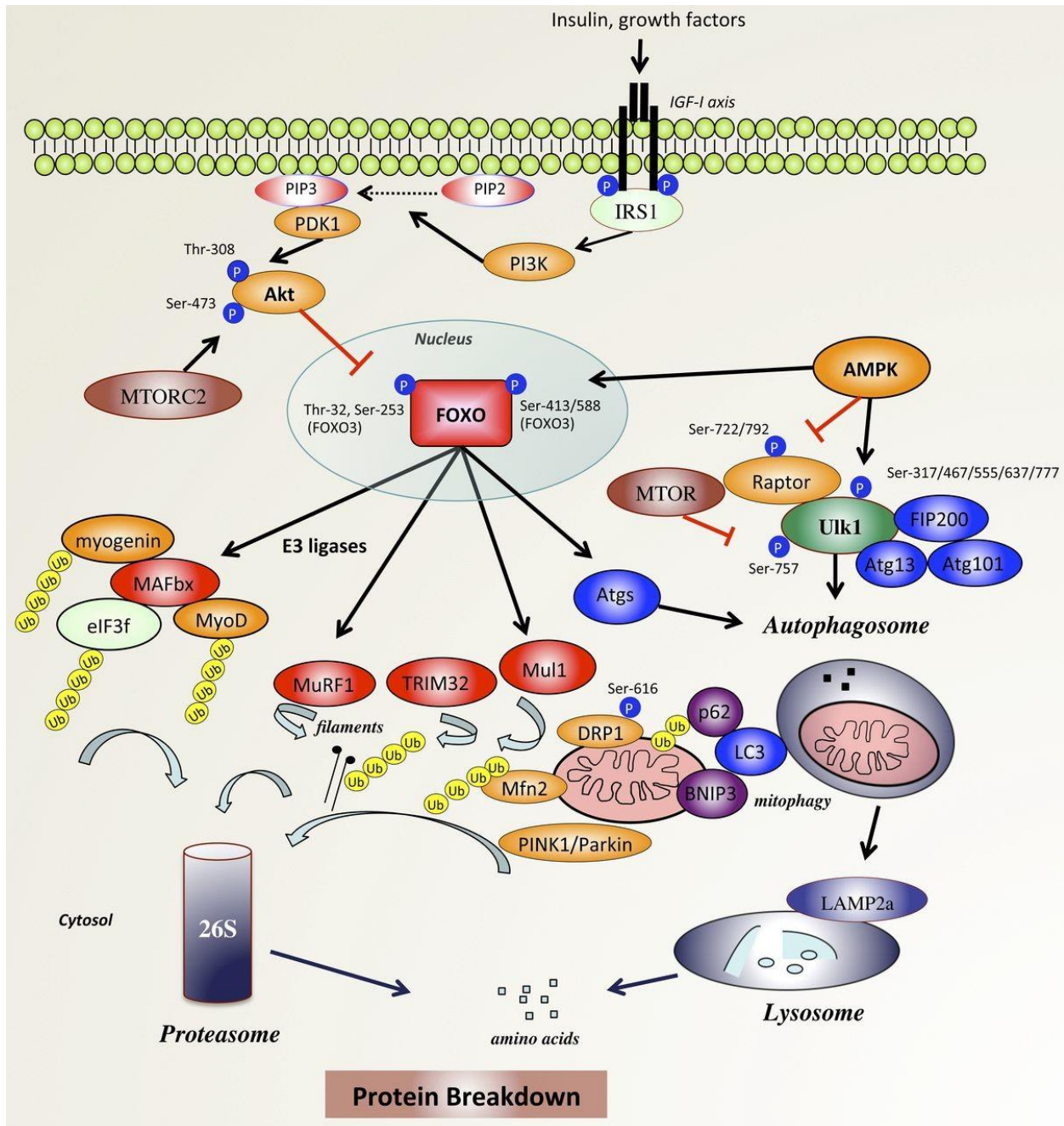
Figure 6: The comprehensive representation of Forkhead box class O proteins (FOXO)-dependent protein breakdown in skeletal muscle. Inhibition of Akt, as a response to growth factor stimulation, phosphorylates FOXO transcription factors. Under conditions of catabolic stress, AMPK phosphorylates and induces FOXO3. As mentioned previously, FOXO factors control the transcription of MAFbx/Atrogin-1 and MuRF1, which are E3 ligases included notably in the

degradation of the eukaryotic initiation factor 3f (eIF3f), MyoD, and myogenin, and several sarcomeric proteins.

TRIM32 is a RING-finger E3 ligase which targets the thin filament components. Moreover, FoxO proteins have a role in increasing the transcription of the mitochondrial E3 ligase Mul1, leading to the ubiquitination, degradation of Mfn2, and mitophagy (selective autophagic elimination of defective mitochondria) during skeletal muscle atrophy. Mitochondrial depolarization stabilizes PINK1 expression, and this leads to the recruitment of the E3 ligase Parkin to damaged mitochondria for mitophagy.

FOXO proteins, also have a role in autophagy, and control the transcription of several atrophy-related genes that have critical roles in autophagosome biogenesis, including LC3. The autophagy adapter p62/SQSTM1 binds directly to LC3 to activate the sequestration of ubiquitinated protein aggregates by autophagosomes. In addition, BNIP3 has a role in mitophagy by binding to LC3 and recruiting the autophagosome to damaged mitochondria. Among atrophy-related genes, ULK1 can induce autophagy initiation and can be phosphorylated by mTOR, leading to its inhibition, and by AMPK, leading to its activation. LAMP2a is a glycoprotein, known for its critical role in autolysosome formation, as illustrated here (Sanchez et al., 2014).

4.4.2.2. IL-6/JAK2/STAT3 pathway in cancer cachexia and muscle wasting

catabolic conditions such as cancer cachexia Increase circulating levels of IL-6 and related cytokines thus inducing STAT3 activity (Zimmers et al., 2016). IL-6 binds membrane receptors and subsequently activates non-receptor tyrosine kinases, such as JAK2. These phosphorylated tyrosine residues recruit STAT3 protein by acting as the intermediary IL-6 signaling. The oncogene STAT3 becomes responsive to extracellular signals and the JAK2 pathway upon activation. After tyrosine phosphorylation, two STAT3 monomers form a dimer, move into the nucleus, and activate gene transcription by binding to specific DNA response elements. IL-6 triggers the activation of the downstream JAK2/STAT3 pathway, which plays a role in promoting tumorigenesis; however, over-expression of STAT3 in tumor cells also triggers the production of IL-6. Therefore, this signaling pathway plays a key role not only in cancer metabolism but also in cancer cachexia. Indeed, IL-6/JAK2/STAT3 signaling pathway is strongly activated in different types of cancer and inhibits anti-tumor activity of immune response as it has been well established by various number of studies (Huang et al., 2022).
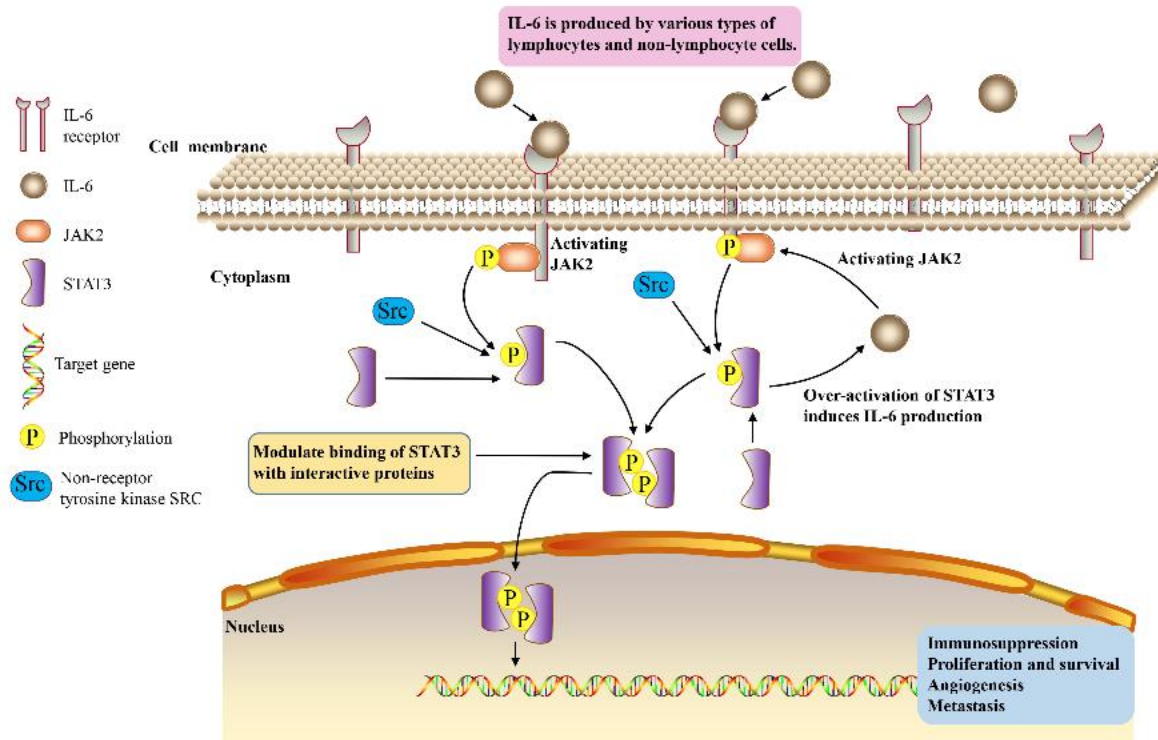
Figure 7: The scheme of the IL6/JAK2/STAT3 pathway (Huang et al., 2022). IL-6 leads to phosphorylation of JAK2. On the other hand, phosphorylated non-receptor tyrosine kinase SRC recruits STAT3 activation. As a loop, the over-activation of STAT3 also leads to the induction of IL-6 production, which activates JAK2.

According to the studies on cancer-associated cachexia, it has been found high association with increased STAT3 localization in myonuclei and observed that IL-6 mediates both the hepatic and skeletal muscle acute phase response via STAT3 activation in cancer (Bonetto et al., 2011). Moreover, activation of STAT3 via IL-6 family ligands has been proved with both *in vivo* and *in vitro* studies. IL-6-induced and tumor-induced mice models indicated activation of STAT3 expression. Transfection of targeted inhibition STAT3 into tibialis anterior muscle tissue of IL-6-induced mice resulted in reduced muscle wasting. *In vitro* model, IL-6-treated C2C12 cells resulted in loss of myofiber diameter and activation of proteasome-dependent STAT3 (Bonetto et al., 2012).

4.4.2.3. TNFα -IKK-Ikβ -NF-kB pathway in cancer cachexia and muscle wasting

The nuclear factor kappa B (NF-κB) transcription factor, which plays a central role in controlling the body's immune response and inflammatory processes, is responsible for the muscle-wasting effects caused by certain inflammatory cytokines, specifically TNF-α and IL6. When NF-κB is inactive, it is kept within the cell's cytoplasm by inhibitory proteins known as Iκβ. When cells are exposed to TNF-α, a signaling pathway is triggered that activates the Iκβ kinase complex (IKK). This complex adds phosphate groups to Iκβ proteins, which marks them for breakdown in the cell through a process called ubiquitination. This degradation of Iκβ frees up NF-κB proteins, allowing them to move into the nucleus of the cell. Once in the nucleus, NF-κB activates genes involved in promoting cell atrophy (Sartori, Romanello, et al., 2021a). In various in vivo research studies, it was presented that the role of TNF-α mediated inflammatory cytokine in response to reactive oxygen species (ROS) is a keystone in muscle wasting, as well as, generation of NF-kB, in response to TNF-α, is the mediator of muscle atrophy (Thoma & Lightfoot, 2018). In the research, NF-kB has been implicated in inhibiting the IGF1 anabolic pathway by interfering the signaling of IGF-1 pathway. In addition, NF-kB inhibits muscle-regulatory factor, MyoD mRNA expression levels upon the induced expression of TNF-α in cancer cachexia conditions (Setiawan et al., 2023). Upon the examination of glucocorticoids (GC) in vivo, methylprednisolone injection had increased the expression of NF-κB-inducing kinase (NIK) which is a significant upstream regulatory kinase controlling NF-κB activation, together with other linchpin muscle catabolic regulators such as Atrogin-1 and MuRF1 that increase muscle proteolysis. Moreover, injection of overexpressed AAV-NIK into tibialis anterior muscle of mice demonstrated a 30% decrease in cross-sectional area of muscle fiber which indicated the association of increased expression of Atrogin-1 and MuRF1 (Fry et al., 2016). Supporting this argument, another research found that overexpression of NF-kB via muscle-specific transgenic expression of increased expression of IKKβ resulted in severe muscle wasting-like clinical cachectic condition, together with an increased ubiquitin ligase MuRF1 expression (Cai et al., 2004).

4.4.2.4. TGF-β/Myostatin/Activin A pathway and BMP/SMAD pathway in cancer cachexia and muscle wasting

The transforming growth factor β (TGF-β) superfamily has been involved in cellular proliferation, differentiation, and growth. The superfamily of TGF-β divides into three categories: TGF-β, bone morphogenetic protein (BMP), and activin. Furthermore, in skeletal muscle, TGF-β, with its related family member myostatin, has been known to have a considerable role in regulating muscle growth (Kollias & McDermott, 2008).

Myostatin, which plays a key role in muscle atrophy in cancer cachexia, is a member of the TGF-β family, excreted by muscle cells and circulating in the bloodstream. Myostatin is known as a negative effector of muscle hypertrophy by hindering the Akt/mTOR pathway and of muscle regeneration with a declined number of satellite cells (Setiawan et al., 2023; Zimmers et al., 2002). On the other hand, myostatin and activin A participate in the same receptor which is activin type II receptor B (ActRIIB) (Setiawan et al., 2023), moreover, ActRIIB intervenes in the signaling of myostatin, activin A, and others from TGF-β family ligands (X. Zhou et al., 2010a). In previous works, it has been found that deletion of ActRIIB resulted in a hypertrophic effect on muscle mass(Lee & McPherron, 2001). In the context of cancer cachexia, it had been demonstrated that blocking ActRIIB pathway in skeletal muscle of C26 tumor-bearing mice reversed the cancer-induced skeletal muscle loss with increased survival rate, without affecting the tumor growth and inhibiting the cancer-induced fat loss (X. Zhou et al., 2010a). In clinical research, it had been also proved a higher circulating level of activin A and myostatin in serum of cachectic patients with lung and colorectal cancer compared to non-cachectic patients (Loumaye et al., 2015).

In the context of the activin/myostatin/TGF-β group, ActRIIB binds to myostatin and activin A, ActRIIA binds to activin A, and TGFβRII binds to TGF-β ligands. These interactions between ligands and their respective receptors ultimately lead to the activation of activin receptor-like kinases (ALK-4, -7, -5), which are a subgroup of receptors involved in the TGF-β signaling pathway. This cascade of receptor interactions reinforces the activation of ALK receptors, facilitating downstream signaling events that regulate various cellular processes.

ALK4/7 and ALK5 phosphorylate Smad2/3, leading to the formation of a Smad2/3–Smad4 heterotrimeric complex. This complex, once activated, remains in the nucleus, where it interacts with other transcription factors, coactivators, or repressors to regulate the transcription of target genes. The other superfamily of TGF-β, BMPs group binds to a complex receptor which combines BMP type II receptor, ActRIIA, and ActRIIB, before reinforcing activation of BMPRIA (ALK3), BMPRIB (ALK6), and ActRIA (ALK2). It is well established that these ligand/receptor groups play a key role in phosphorylation, hetero-trimerization, and transcriptional regulation effectiveness of Smad/1/5/8 with Smad4 (Sartori et al., 2014). It had been found that Smad3 itself was sufficient to overcome atrogin-1 activity by inhibiting Akt/mTOR signaling pathway that leads to muscle atrophy (Goodman et al., 2013). Moreover, inhibited Smad2/3 was observed to induce muscle hypertrophy with dependency on mTOR signaling pathway (Sartori et al., 2009). On the other hand, it had been found that the BMP/Smad1/5/8 axis is positively associated with muscle growth, and activation of BMP via targeting its receptor and Smad1/5/8 downstream transcription factors was effective in preventing muscle atrophy and inducing the hypertrophy(Sartori et al., 2013). Subsequently, Sartori et. al. reported that Noggin expression, which is known as an extracellular inhibitor of the Smad1/5/8 signaling pathway, is triggered by cancer-mediated factors such as Activin A and IL-6, leads to BMP inhibition in skeletal muscle, consecutively causing muscle wasting, impairment in neuromuscular junction morphology and function (NMJ). Subsequently, they found that reactivating BMP signaling in the muscles of tumor-bearing mice is sufficient to protect skeletal muscle wasting in presence of the tumor (Sartori, Hagg, et al., 2021).
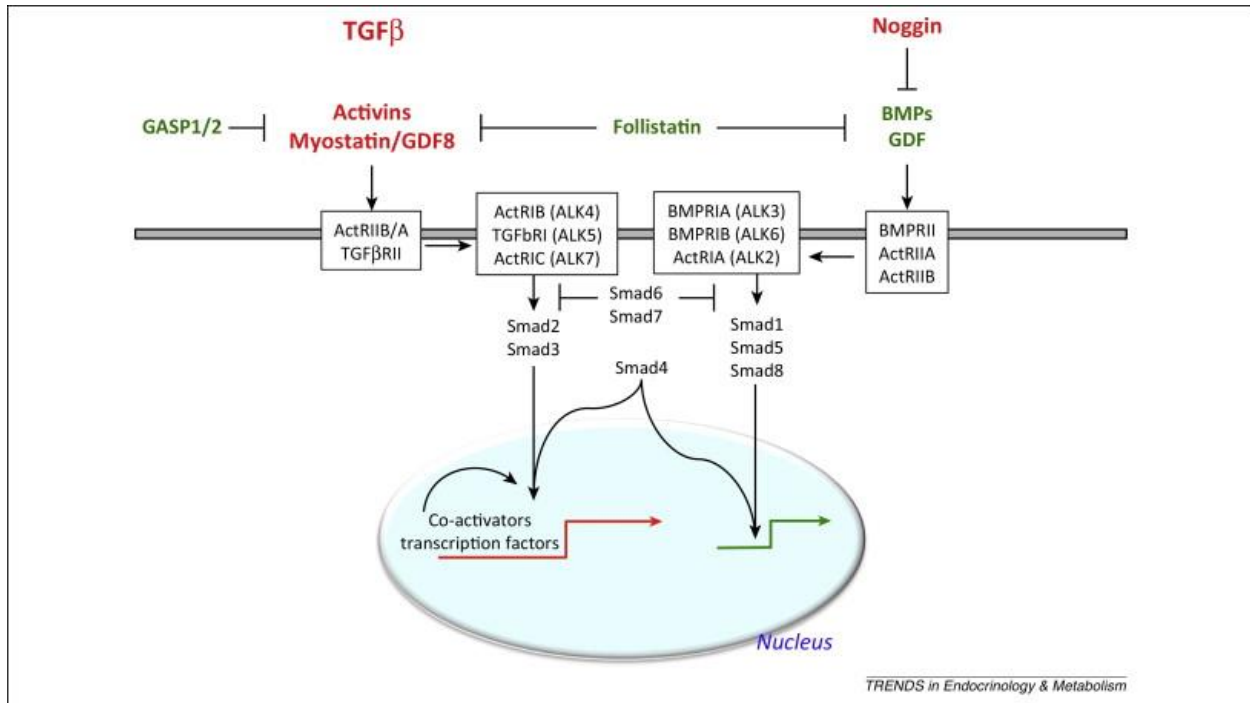
Figure 8: The scheme of signaling and crosstalk pathways between myostatin [growth and differentiation factor 8 (GDF8)]/activin/transforming growth factor beta (TGFβ) and bone morphogenetic protein (BMP)/GDF subfamilies. The red indicators show the leadings of protein degradation, and the green indicators show the leadings of protein synthesis. Myostatin (GDF8)/activin/TGFβ activates Smad2/3, whereas the BMP/GDF subfamilies activate Smad1/5/8. Smad4 is a cofactor that is shared by the usage of different Smad proteins and is required for transcriptional activity at the target genes (Sartori et al., 2014).

4.4.2.5. Inflammatory mediators that play a key role in cancer cachexia-related tissue wasting

It is well established that chronic inflammation is observed in carcinogenesis, and cancer cells exploit the production of proinflammatory mediators for growth, protection from apoptosis, and promotion of angiogenesis. These proinflammatory mediators, also called proinflammatory cytokines, have been highly involved in tumor-induced adipose and skeletal muscle loss (K. C. H. Fearon et al., 2012). Among these factors, in the context of cancer cachexia proinflammatory cytokines, particularly TNF-α, IL-6, IL-1α, and β, are very well studied inflammation players (Schmidt et al., 2018a).

One of the main proinflammatory cytokines is TNF-alpha (TNF-α); TNF-α has been shown to have a role in the activation of a cycle between fructose-6-phosphate and fructose 1,6-biphosphate which elevates glycolytic activity and leads to increased energy expenditure, heat production, and tissue wasting (Rohm et al., 2019).

In previous research studies, it has been proved that TNF- α is one of the induced cytokines in cachectic mice, and it inhibits the maturation of adipocyte and skeletal myocytes in vitro (K. C. H. Fearon et al., 2012). In other studies, it has been also observed that engrafting tumor cell lines, which continuously produce TNF-α, into mice has triggered cachexia and weight loss with reduced food intake, compared to the control group (Oliff et al., 1987; Webster et al., 2020). Additionally, in another study, it has been observed that TNF-α has a role in suppressing the IGF-1 pathway and resulting in insulin resistance, thereby explaining its activity in dysregulation and impaired utilization of macronutrient uptake (Webster et al., 2020). In addition to that, since cancer cachexia is a condition featuring alteration of macronutrient metabolism, TNF-α is also responsible for enhancing gluconeogenesis, adipose tissue loss, lipid mobilization, and downgrading glycogen and lipid synthesis (Patel & Patel, 2017).
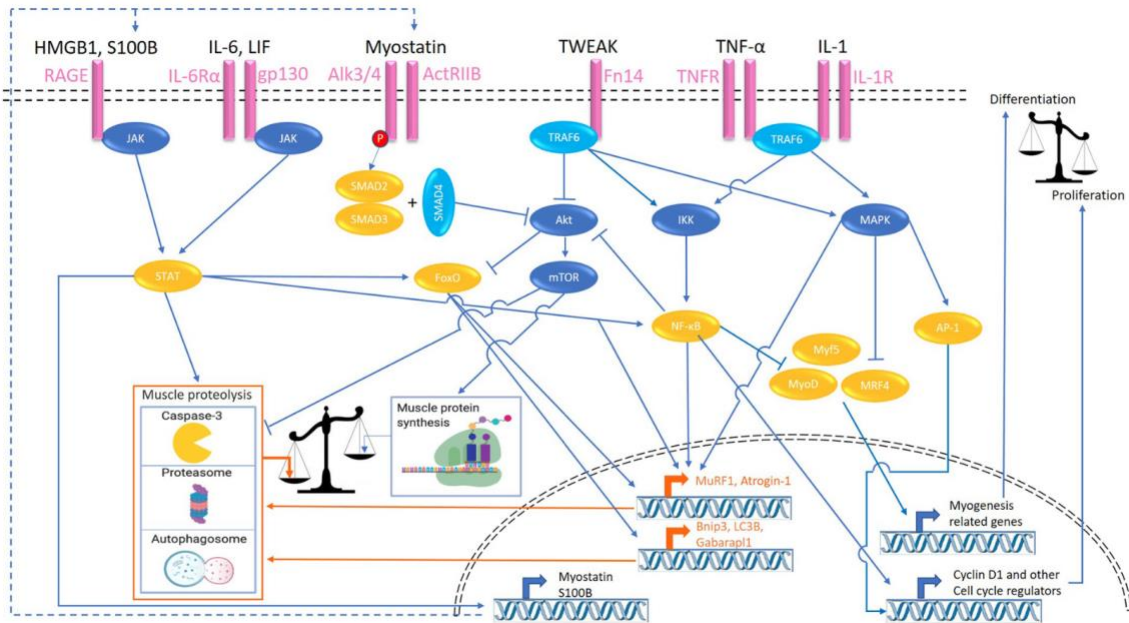
Figure 9: The scheme of signaling pathways activated by inflammatory factors that take place in cancer cachexia-induced muscle atrophy (Webster et al., 2020). Colors refer to transcription factors (orange), proteolytic signaling (orange), kinases (dark blue), adaptor proteins (light blue), and cell surface receptors (pink). HMGB1, high mobility group box 1; S100B, S100 calcium-binding protein B; RAGE, the receptor for advanced glycation endproducts; ActRIIB, activin receptor type IIB; TWEAK, tumor necrosis factor-like weak inducer of apoptosis; Fn14, fibroblast growth factor-inducible 14; TNF-α, tumor necrosis factor-α; IL, interleukin; JAK, Janus kinase; STAT, signal transducers and activators of transcription; TRAF, TNF receptor-associated factor; FoxO, Forkhead box transcription factors; mTOR, mammalian target of rapamycin; IKK, IκB kinase; NF-κB, nuclear factor-κB; MAPK, mitogen-activated protein kinase; JNK, c-Jun N-terminal kinase; MyoD, myoblast determination protein 1; MyoG, myogenin; MRF4, myogenic regulatory factor; AP-1, activator protein 1; MuRF-1, muscle RING-finger protein-1; Bnip3, BCL2 interacting protein 3; Gabarapl1, GABA type A receptor-associated protein-like 1.

The other main proinflammatory cytokine that is induced as a result of cachexia is IL-6. In cancer patients, it has been shown that circulating levels of IL-6 associate with weight loss and reduced survival (K. C. H. Fearon et al., 2012). In the promotion of tumor growth and metastasis, IL-6 also plays a key role as a result of chronic inflammation and the development of cancerous tissue by resulting in skeletal muscle atrophy, protein breakdown, and development of cachexia (Paval et al., 2022).

In terms of the importance of IL-6 in tissue wasting of cancer-associated cachexia, one recent study has observed that tumor-bearing mice, inoculated with IL-6 knock-out (KO) CHX207 fibrosarcoma cancer cells, have been protected from total body weight loss as well as loss of skeletal muscle and adipose tissue mass compared to non-deleted CHX207-tumour-bearing mice (Pototschnig et al., 2023).

Among proinflammatory interleukins, not only IL-6 but also elevated circulation levels of IL-8, IL-10 and IL-1 receptor antagonist (IL-1RA) have been found in patients with pancreatic carcinoma which result in weight loss and reduced reaction to treatments (Ebrahimi et al., 2004).

The fibroblast growth factor-inducible 14 (Fn14) receptor responds to growth factors and proinflammatory cytokines, including TNF-like weak inducer of apoptosis (TWEAK), a member of the TNF superfamily ligand. Upon binding with TWEAK or other relevant ligands, Fn14 is activated, thereby initiating TNF signaling. This interaction plays a crucial role in mediating cellular responses to growth factors and proinflammatory cytokines. The TWEAK-Fn14 axis has a prominent role in muscle atrophy and muscle regeneration by impacting myoblast proliferation and differentiation (Tajrishi et al., 2014). In one study, TWEAK-Fn14overexpression has been observed in C26 cells, and using antibodies against Fn14, causes an increase in mice survival and reduction of tumor-induced weight loss (Johnston et al., 2015).

Growth differentiation factor – 15 (GDF-15) which is also a member of the TGFβ superfamily, has established its role several pathological conditions, such as cancer and cardiovascular diseases (Rohm & Herzig, 2020; Tsai et al., 2018). GDF-15 acts through a receptor which is called glial-derived neurotrophic factor (GDNF) receptor alpha-like (GFRAL). GFRAL is known as a distant

orphan member of the GDNF receptor family which signals through the tyrosine kinase receptor pathway (Tsai et al., 2018).

GDF15-GFRAL signaling axis has been well studied in cancer-related cachexia field. Elevated circulating levels of GDF15 have been seen as one of the causes of anorexia, and recombinant forms of this protein have been observed as effective in triggering weight loss in mice (Rohm & Herzig, 2020). Moreover, it has been indicated that engineered prostate cancer cell lines overexpressing GDF15 tumor-bearing mice lost a significant amount of weight, fat mass, and lean mass, and induced cachexia/anorexia (Tsai et al., 2018). On the other hand, GDF15 knock-out mice showed an increase in weight, adiposity, and food intake independently on the presence of the tumor (Tsai et al., 2013).

In addition, a signaling complex, known as GFRAL-Ret proto-oncogene, that is located in brainstem neurons mediates GDF15-induced weight loss in mice. In a recent study an antagonistic antibody 3P10, which targets and inhibits GFRAL-Ret proto-oncogene signaling pathway, showed decreased reactive lipid oxidation in tumor-bearing mice by leading to prevention of cancer-related cachexia (Suriben et al., 2020). Those findings suggest that the GDF15-driven signaling axis could have a significant role in the prevention and treatment of cancer cachexia (Rohm & Herzig, 2020; Suriben et al., 2020).

4.4.3. Adipose tissue depletion in cancer-related cachexia

It has been well established that tumor-bearing rodent models demonstrated increased lipid utilization and adipose tissue wasting as well as increased turnover of glycerol and free fatty acids circulation in cancer patients due to elevated lipolysis (Rohm et al., 2019; Tisdale, 2009). It has been observed that adipose tissue wasting occurs before the reductions in skeletal muscle mass and food intake in the experimental cachexia models both in rodents and in cancer patients (Dalal, 2019).

Lipolysis is based on the enzymatic activity of three lipases: adipocyte triglyceride lipase (ATGL), hormone-sensitive lipase (HSL), and monoglyceride lipase (MGL) (Rohm et al., 2019). In many studies, it has been demonstrated that mRNA expression of ATGL and HSL heightened in lipolysis in subcutaneous white adipose tissue (WAT) which has a significant correlation with elevated triacylglycerol (TAG) and free fatty acids (FFA) levels as well. Indeed, blocked expression of these lipases indicated partial protection from WAT lipolysis (Dalal, 2019). Moreover, chemokines such as IL-6 and TNF-α have an important role in the induction of lipolysis and overall wasting in cachexia conditions (Vegiopoulos et al., 2017), as it had been found that IL-6 receptor inhibition repressed not only WAT wasting but also browning of WAT in cachectic mice (Han et al., 2018).

Another accountable reason for increased energy expenditure in cancer cachexia is increased level of beige (browning) adipose tissue leading to increased thermogenesis (Vegiopoulos et al., 2017). It had been reported that colorectal tumor-bearing mice demonstrated increased level of uncoupling protein-1 (UCP1) with activated thermogenesis (da Fonseca et al., 2020). Also, Kir et al. reported that inhibiting tumor-derived parathyroid-hormone-related protein (PTHrP), which has been known for its regulatory impact on adipose tissue thermogenesis, contributed to the maintenance of muscle and fat mass even though increased tumor size in Lewis lung carcinoma (LLC) tumor-bearing mice (Kir et al., 2014). Although the role of both white and brown adipose tissue needs to be further elucidated, those findings give valuable contributions in the context of understanding metabolic impairment in cancer cachexia.

4.5. Exploring Novel Approaches for Targeted Treatment of Cancer Cachexia

Cachexia-associated cachexia prevalence is as common as 87% in pancreatic and gastric cancer patients, 61% in colon, lung, and prostate cancer patients and non-Hodgkin lymphoma, and 40% in breast cancer patients, sarcoma, leukemia, and Hodgkin lymphoma. Cachexia corresponds up to 30% of all cancer-related deaths, and accounts for incremental systemic inflammatory response, catabolism, involuntary loss of body mass as well and impaired nutritional intake (Ni & Zhang, 2020a), none the less, there are no current therapeutic agents that have been developed and used for treatment against to cachexia and/or cancer-associated cachexia (Kasprzak, 2021). Nevertheless, an advanced understanding of the molecular and genomic mechanisms of cancer cachexia could lead to novel targeting improvements in the various stages of treatment and drug development (Kadakia et al., 2023).

Manipulating the expression of catabolic pathways by counteracting protein degradation and triggering protein synthesis emerges as a potential treatment to overcome skeletal muscle wasting of cancer-associated cachexia. It has been highlighted the importance of myostatin and activin-A pathways in tumor-induced muscle since the inhibition of their expression and sub-pathways resulted in the prevention of skeletal wasting and increased survival (Setiawan et al., 2023).

On the other hand, high-throughput omics-based technologies allow the discovery of molecular profile alterations of skeletal muscle wasting in cancer cachexia to have better insights of cancer-derived cachexia (Gilmore et al., 2023).
Conventional methods of high-throughput transcriptomics analyses, such as bulk RNA sequencing and single-cell RNA sequencing allow us to examine gene expression differences during disease by averaging gene expression level from all cells within a tissue or by discriminating cell populations from the tissue; however, even though these methods are valid, they don't provide

information about the gene expression location of cells within the tissue with consideration of cellular heterogeneity. Therefore, spatial transcriptomics unravels the discovery of cellular function in a spatial context within tissue in the progress and development of disease and provides a broader picture of underlying mechanisms of biological systems with the ultimate goal of developing new therapeutic findings and applications (R. Zhou et al., 2023).

5. Aim of the work

Based on the previous research that has been conducted in our laboratory and our comprehensive understanding of the molecular mechanism underlying muscle atrophy in cancer-associated cachexia, it is firmly established that MuRF1 and FoxO1/3 play a crucial role in the muscle protein degradation process. Their expression increases significantly in the context of cancer-associated cachexia-induced muscle atrophy. Targeting and investigating these proteins in detail heralds the promise of advancing the field of cancer cachexia research.

Our first objective is to simultaneously knock down MuRF1, FoxO1 and FoxO3 using RNA interference plasmid constructs and injecting them into the muscle tissue of C26 tumor-bearing mice. We hypothesized that blunting the expression of genes that have an important role in mediating the atrophic program that leads to muscle wasting condition in cancer-associated cachexia, could prevent muscle mass wasting and be a novel RNA-based targeted treatment approach in the field.

Our second goal is to investigate the molecular profiles and the transcriptional activities of genes in distinct spatial locations within muscle tissue affected by cancer-associated cachexia by using the spatial transcriptomics method. Moreover, this cutting-edge methodology allows us to distinguish mRNA profiles resulting from targeted knockdown of MuRF1, FoxO1, and FoxO3 in cancer-cachectic muscle tissue, in contrast to a control group. Ultimately, this approach will enable us to uncover gene and protein expressions, and cell-to-cell communication at a subcellular resolution by specifically sampling the tissue where the targeted atrophic genes in cancer-induced muscle tissue have been knocked down.

The overarching objective of these experiments is not only to develop a novel combinatorial RNA-based targeted treatment for muscle wasting associated with cancer-associated cachexia but also

to elucidate and discover novel transcriptional activities resulting from the application of this RNA-based targeted treatment in this context.

6. Material and Methods

6.1. Animal Experiments and Preparation of Cachexia Animal Models

The *in vivo* experiments adhered to ethical guidelines for the care and use of animals in scientific research. All experimental protocols received approval from the Italian Ministry of Health, specifically under Office 5 with authorization number 1060/2015 PR. Surgical procedures, including tumor inoculation and plasmid injection, were carried out with animals under isoflurane inhalation in medical oxygen, and post-operative pain relief was provided through tramadol analgesia. The animals were provided with standard chow diets and had unrestricted access to drinking water while being housed in a controlled environment with a 12-hour light-dark cycle. Littermates of the same sex were randomly assigned to experimental groups.

6.2. Culture and inoculation of colon-26 (C26) carcinoma tumor cell lines

The mouse colon-26 (C26) carcinoma cell line is derived from the tumor tissue of Balb/c mice bearing C26 carcinoma. As previously described (Geremia et al., 2022), C26 cells were grown in high glucose DMEM (Dulbecco's Modified Eagle Medium, (#41966 Gibco). To support their growth, all culture media were enriched with 10% fetal bovine serum (Gibco) and a Pen/Strep solution (containing penicillin at 100 U/ml and streptomycin at 0.1 mg/ml, Gibco). The cells were consistently maintained at 37°C in a controlled environment with 5% CO_2 to ensure proper incubation conditions. Throughout the experiments, low-passage cell lines were employed.
C26 cells' suspension, which are purified and preserved in PBS, were subcutaneously injected into the dorsal region of ~8-week-old Balb/c strain mice. Each tumor-bearing mouse received 5 x 10^5 C26 cells with an inoculation of 100ul in a physiological solution. In all the experimental models of cancer cachexia, the mice received treatment until they reached the experimental endpoint,

which was determined based on ethical considerations and defined as a ~20% loss of their initial body mass and ~15% loss of their initial lean mass. In consequence, tumor-bearing mice were euthanized when they reached a defined experimental endpoint which is typically around 15 days after inoculation. Body composition analysis in mice was performed by quantitative magnetic resonance imaging (using an EchoMRI) without being anesthetized.

6.3. RNA-interference experiments *in vitro* and *in vivo*

6.3.1. Designing of MuRF1 targeting sequence and cloning shMuRF1 via BLOCK-iT Pol II miR RNAi Expression Vector Kit with EmGFP

To create RNAi-mediated knockdown of MuRF1, shRNA against MuRF1 was cloned via BLOCK-iT Pol II miR RNAi expression vector pcDNA 6.2 GW/EmGFP-miR. This vector system is specifically designed to clone double-stranded oligo duplexes encoding a desired miRNA target sequences and contains specific miR flanking sequences that allow proper processing of the miRNA. Moreover, EmGFP (Emerald Green Fluorescent Protein) is incorporated into the vector in such a way that the pre-miRNA insertion site is in the 3' untranslated (3'UTR) region of the fluorescent protein mRNA.

The knockdown of the target gene correlates with the EmGFP expression. The miRNA generated by Block-iT fully complements their target size and cleaves target mRNA (Figure 10).
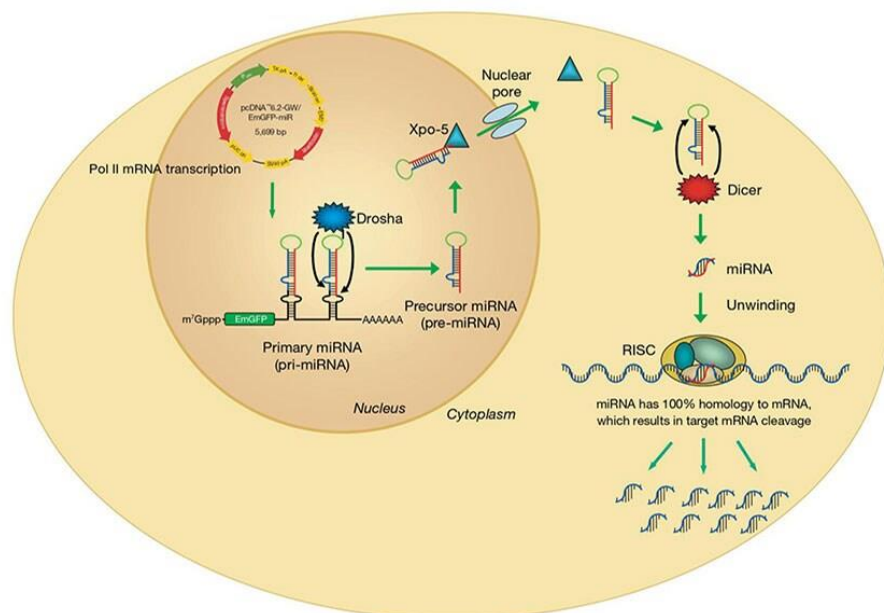
Figure 10: The BLOCK-iT™ Pol II miR RNAi Expression System

In the designing of targeting gene of interest (shMuRF1) sequence via pcDNA 6.2-GW/± EmGFP-miR vectors, an engineered pre-miRNA sequence has been used based on the murine miR-155 sequence, and 5' and 3' flanking regions derived from the miR-155 transcript were inserted in the vector. The pcDNA 6.2-GW/EmGFP-miR is supplied with a linearized vector, thus it brings the necessity of containing specific 4 nucleotide 5' overhangs on each strand for directional cloning (Figure 11).
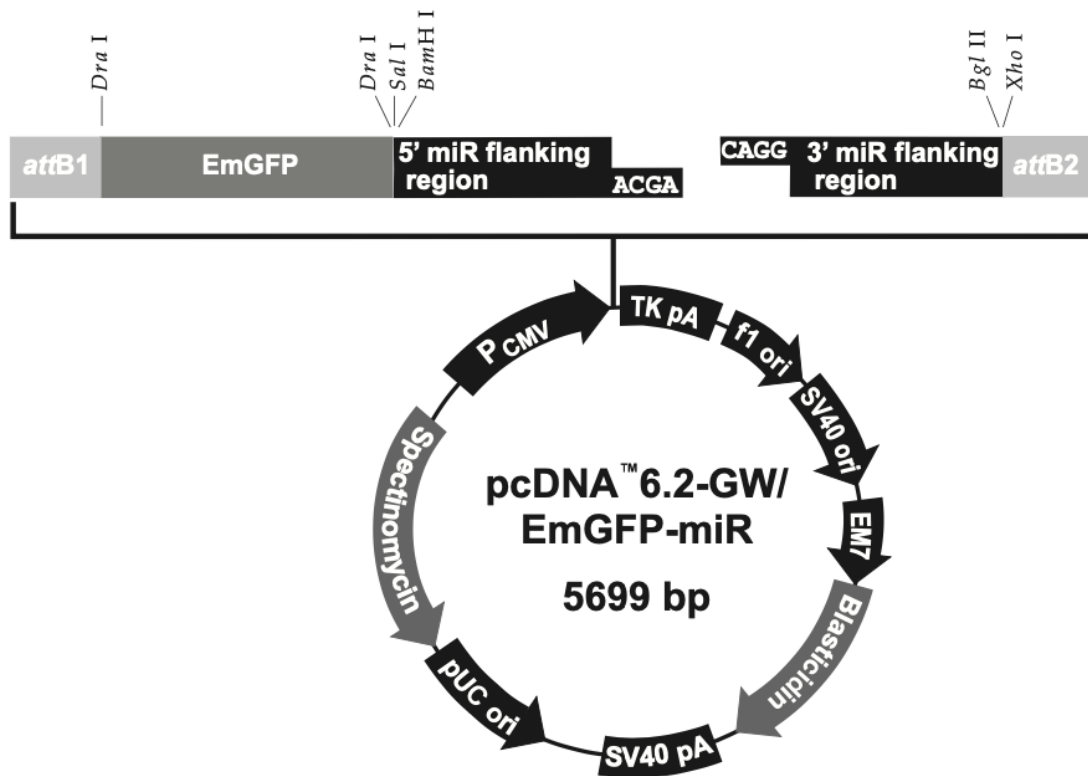
Figure 11: The BLOCK-iT™ Pol II miR RNAi Expression vector

Following the steps, as instructed, single-stranded complementary DNA oligos were designed and synthesized. Annealing steps are completed to generate double-stranded (ds) DNA oligos, consecutively, ligation and bacterial transformation experimental steps were conducted for cloning shRNA against MuRF1.

6.3.2. Designing of FoxO1/3 targeting sequence and cloning FoxO1/3 via pSUPER RNAi vector system

The RNAi-mediated targeting knocking down expression of both FoxO1 and FoxO3 sequences was designed, and cloned via the pSuper RNAi vector system, previously in our lab. The pSUPER RNAi system is used to design oligonucleotides with a 19-nucleotide target sequence which is derived from the mRNA transcript of the targeted gene for knocking down.

In the following steps, single-stranded complementary DNA oligos were designed and synthesized. Annealing, ligation, and bacterial transformation experimental steps were conducted for cloning our gene of interest.

6.4. Plasmids and Antibodies

The constructs used during *in vivo* electroporation experiments: shFoxO1/3 (previously validated by the lab) was cloned via pSuper RNAi System, while shMurF1 and sh-scrambled oligos were cloned using BLOCK-iT Pol II miR RNAi Expression Vector Kit with EmGFP (Thermo Fisher Scientific).

Target sequences of RNAi plasmids:

• shFoxO1/3 - GGATAAGGGCGACAGCAAC

• shMuRF1 460 - TGATTCCTGATGGAAACGCTA

• shMuRF1 461 - GGAGAATAGCCACCAGGTGAA

• shMuRF1 462 - GACCACAGAGGGACACCAATA

• shMuRF1 463 - CGAGTGCAGACGATCATCTCT

• sh-scrambled - GTCTCCACGCGCAGTACATTT

The following antibodies from Santa Cruz Biotechnology were used: antibody to GFP (sc-8334). Mouse monoclonal antibodies to Flag (M2; F3165) were purchased from Sigma. Mouse monoclonal antibody to GAPDH (ab8245) was purchased from Abcam.

6.5. RNAi *in vitro*

6.5.1. Culture of C2C12 mouse myoblast cells and transfection experiment

For the efficiency validation of knocking-down shMuRF1 construct, which has been cloned via BLOCK-iT, C2C12 mouse myoblast cell lines were purchased from ATCC, and were cultured in DMEM medium (Gibco–Life Technologies) supplemented with 10% fetal bovine serum (Gibco) and 1% Pen/Strep solution (penicillin 100 U/ml and streptomycin 0.1 mg/ml, Gibco), and incubated at 37 °C with a humidified atmosphere of 5% CO_2 until cells reached enough confluency. Transfection of shMuRF1 into the cells was conducted via Lipofectamine 2000 Transfection Reagent (Life Technologies) by following the instructions. Cell lines used in the experiments were authenticated and tested for mycoplasma contamination. Throughout the experiments, low-passage cell lines were employed.

6.6. RNAi *in vivo*

6.6.1. *In vivo* transfection experiment

In vivo transfection experiments were conducted by injecting intramuscular expression plasmids into the tibialis anterior (TA) muscle, followed by electroporation.

Transfections were conducted on the same day of C26 cells inoculation and mice were euthanized after ~15 days, as described when they reached the experimental endpoint.

Transfection procedure was previously described (Bonetto et al., 2012). Before starting transfection, mice were anesthetized with Tribromoethanol (Avertin) or isoflurane, continuously legs were shaved and positioned to facilitate easy access to the TA muscle.

20 µg of individual plasmid vectors, encoding shMuRF1 and sh-pan-FoxO (FoxO1 and FoxO3), prepared in physiological salt solution, were administered into one tibialis anterior muscle using the syringe.

One minute after intramuscular injection of the plasmid, transcutaneous pulses were implemented by 2 stainless steel plate electrodes. Five pulses (20 m/sec pulse length with 200 ms pulse interval) were administered to the muscle with a delivery rate of 21 volts.

6.7. qRT-PCR

Total RNA was extracted from frozen skeletal muscle tissue using TRIzol (Life Technologies) and the Tissue Lyser II with the following RNA extraction steps. The RNA concentration was measured using a Qubit 2.0 Fluorometer (Invitrogen). 1 µg of extracted RNA was reverse transcribed using reverse transcriptase (Multiscribe, Thermo Fisher Scientific). mRNA levels were analysed by quantitative Real-Time PCR. All data were normalized to either Gapdh or Actb gene expression using the ddCt method. The sequences of the oligonucleotide primers used are listed in the table listed below.

Table: Primers used to analyse quantitative RT-PCR.

Target	Forward primer	Reverse primer
mMuRF1	ACCTGCTGGTGGAAAACATC	CTTCGTGTTCCTTGCACATC
mGaphd	CACCATCTTCCAGGAGCGAG	CCTTCTCCATGGTGGTGAAGAC
mActb	CTGGCTCCTAGCACCATGAAGAT	GGTGGACAGTGAGGCCAGGAT

6.8. Western Blotting

To obtain C2C12 protein lysates, cells were homogenized in lysis buffer containing 50 mM Tris, pH 7.5, 150 mM NaCl, 5 mM MgCl2, 10% glycerol, 1% SDS, 1% Triton X-100 and phosphatase (P5726, Sigma) and protease (P8340, Sigma) inhibitors. Protein fractions were resolved by SDS-PAGE using pre-cast 4-12% Bis-Tris gels (Thermo Fisher Scientific), blotted onto nitrocellulose or PVDF membranes (BioRad, Merck), and incubated with the appropriate primary antibody overnight. Protein detection was performed as previously described (Winbanks et al., 2011). Blots were stripped either by 20 min incubation in boiling water at 80°C or by 2x10 min washes in mild stripping buffer containing 0.2 M Glycine, 0.1% SDS, 1% Tween-20, pH 2.2.

6.9. Cross-sectional area (CSA) analyses of muscle fibers

For cross-sectional area analyses, a series of 10 μm TA muscles' cryosections were obtained from the mid-belly of the muscles in the cryostat. Cryosections of transfected and untransfected TA muscles' fibers were examined in the microscope via fluorescence signals. Transfection efficiency has been assessed by checking enhanced green fluorescent protein (EGFP) signal. Cross-sectional areas of muscle fibers were measured by using the ImageJ.

6.10. Preparation of muscle slides for spatial transcriptomics analyses

For spatial transcriptomics experiment, we used male mice. Mice were categorized as non-tumor-bearing mice (Sham), C26 tumor-bearing mice and C26 tumor-bearing mice transfected with shMuRF1 and shFoxO1/3 constructs in TA.

When mice were euthanized in the experimental endpoint, they were dissected, and muscles were taken. For formalin-fixed paraffin-embedded (FFPE) muscle tissues preparation for spatial transcriptomics analysis, muscles were fixed with 10% Neutral Buffered Formalin (NBF) for 7h, 12h, and 24h respectively on the rotator at room temperature. As a continuation, samples were preserved in an ethanol 70% solution at 4°C. The tissues were then included in paraffine and cut in 10 μm thick sections at the microtome and placed onto Superfrost® Plus Microscope Slides.

In order to preserve RNA integrity and physiological muscle structure, we proceed with 12h 10% NBF fixed TA muscle tissues for further analyses.

6.11. Histological staining

6.11.1. Hematoxylin and Eosin staining on Formalin-Fixed Paraformaldehyde Embedded (FFPE) skeletal muscle tissue

Hematoxylin and eosin staining was implemented on prepared skeletal muscle tissues as previously described (Winbanks et al., 2016). This staining was used for the examination of FFP-embedded skeletal muscle tissues morphology. Hematoxylin and Eosin reagents were applied on muscle section slides respectively, and mounted with Eukitt mounting medium, and images were captured on a Leica DM6B fluorescence microscope.

6.11.2. Immunofluorescence staining on Formalin-Fixed Paraformaldehyde Embedded (FFPE) skeletal muscle tissue

For the Immunofluorescence staining, 12h-fixed with 10% NBF, 10 µm muscle sections were considered. 10x Genomics Visium Spatial Gene Expression for FFPE Deparaffinization, Decrosslinking, Immunofluorescence Staining & Imaging – CG000410 | Rev D protocol was used, and the workflow for deparaffinization, decrosslinking, and antibody staining have been applied respectively.

The primary antibody used for immunofluorescence is rabbit anti-GFP (sc-8334) (1:100) incubated for one hour at room temperature. To highlight fibers' membrane, the sections were then stained with AlexaFluor 555 conjugated Wheat Germ Agglutinin (WGA, Thermo Fisher Scientific) (1:200) in phosphate buffered saline (PBS) for 1 hour at 37°C. Afterwards, sections were incubated with Alexa fluor 488 anti-rabbit (Jackson 111-145-144). For nuclear staining, sections were incubated with DAPI solution in PBS for 5 minutes at room temperature. In the end, they were washed in PBS and mounted with a mounting medium for microscopical visualization via Leica DM6B fluorescence microscope.

6.12. RNA extraction, integrity check, library preparation and preprocessing for Spatial Transcriptomics Analyses

RNA was extracted from 20 slices of 10 µm using Qiagen RNeasy FFPE kit and RNA integrity was checked by RNA 6000 Pico Kit (Agilent). Spatially tagged cDNA libraries were built using a Visium Spatial Gene Expression 3 Library Construction v1 Kit (10x Genomics, PN-1000187; Pleasanton, CA).

Preprocessing of raw spatial transcriptomics data, including library generation, sequencing and spots distribution across the tissue were conducted via Space Ranger analysis software (10x Genomics, Visium Spatial Gene Expression for FFPE assay) (*Space Ranger - Official 10x Genomics Support*, n.d.).

Analysis of sample quality was performed based on the following criteria: number of reads, valid barcodes, valid UMIs, sequencing saturation, Q30 bases in the barcode, Q30 bases in probe read, Q30 bases in UMI, number of spots under tissue, mean reads per spot and median genes per spot.

Table: Interpretation of the metrics parameters for Visium Spatial Gene Expression for FFPE library assay via Space Ranger tool

Metrics (Sequencing & Spots)	Definements/ Indications
Number of reads	Total number of read pairs, assigned to the library.
Valid barcodes & Valid UMIs	Fraction of reads, and low valid barcodes (<75%) might indicate sequencing issues.
Sequencing saturation	The fraction of reads originating from an already-observed UMI. This indicates a function of library complexity and sequencing depth.
Q30 bases in barcode/UMI & Q30 bases in probe read	Fraction of tissue-associated barcode. Low Q30 base percentages might indicate sequencing issue (e.g. sub-optimal loading concentration)
Fraction reads in spots under tissue	The fraction of valid barcode. It indicates the mapping to transcriptome reads with tissue-associated barcodes. Being >50% indicates efficient RNA permeabilization and many of the reads ideally assigned to tissue covered with spots.
Mean reads per spot	The number of reads within the tissue. Optimally, 25.000 reads per spot minimum recommended
Median genes per spot	The median number of genes detected per tissue covered with spots. Lower than expected might indicate low sequencing depth, library complexity or quality.

6.13. Statistical Analyses

Statistical tests (Student's t-tests or Mann-Whitney, two-way ANOVA with Benjamini, Krieger, and Yekutieli adjustment) were implemented as described in the figure legends. They were conducted upon verification of the normality assumption using the Kolmogorov-Smirnov test. Data are presented as means ± SEM in the graphs. Differences between groups were considered statistically significant if the P value was less than 0.05; the P values are reported in the figure legends. All the n reported in the figure legends refer to biological replicates. Every experiment was replicated at least twice. Animal cohorts were repeated to establish confidence in the reproducibility of the data presented. Initial optimization of experimental reagents such as dose-response experiments was performed. Statistical analyses were performed using GraphPad Prism 7.0a (GraphPad).

7. Results

7.1. The expression of MuRF1 is knocked down in cells (*in vitro*) and muscle (*in vivo*)

To obtain the knockdown of MuRF1 through RNA interference, shRNA construct against MuRF1 was cloned via BLOCK-iT Pol II miR RNAi expression vector pcDNA 6.2 GW/EmGFP-miR (Life Technologies). This co-cistronic vector, similar to pcDNA6.2™-GW/miR, incorporates the coding sequence of EmGFP (Emerald Green Fluorescent Protein) into the vector, placing the pre-miRNA insertion site in the 3' untranslated (3'UTR) region of the fluorescent protein mRNA. EmGFP facilitates the tracking of miRNA/shRNA expression and establishes a strong correlation between EmGFP expression and the knockdown of the target gene by the miRNA/shRNA.

Four distinct oligos (#460, #461, #462, #462) against MuRF1 were cloned into the vector in order to identify the most efficient one in knocking down MuRF1 levels. The knocking-down validation of the four tested oligos was examined in C2C12 cells *in vitro via lipofectamine transfection*. The different shRNA-mediated knockdown efficiencies of overexpressed Flag-MuRF1 were validated via immunoblotting (Figure 12A). Based on the *in vitro* results, the most effective shRNA construct (#461) in reducing MuRF1 protein levels was selected for *in vivo* experiments.

The selected shRNA construct against MuRF1, oligos #461 cloned in the co-cistronic vector encoding GFP as described above, was transfected into the tibialis anterior (TA) muscle tissue of rodent model via electroporation in order to evaluate the knock-down of MuRF1 mRNA expression level *in vivo*. As a negative control, scrambled oligos were transfected. Two weeks later, TA muscles were collected, RNA was extracted, and endogenous MuRF1 transcript levels were quantified using real-time PCR. According to the result, the shRNA construct against MuRF1 oligos (#461) efficiently knocked down the MuRF1 transcript level in TA muscle tissue compared to the

negative control (Figure 12B). For this reason, this construct was continually used for further experiments.
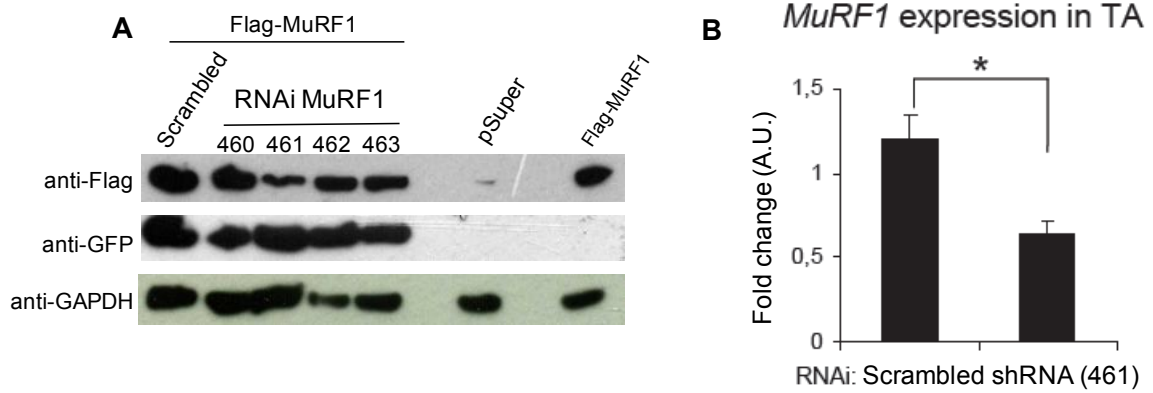
Figure 12: (**A**) RNAi-mediated knockdown of MuRF1 revealed by immunoblotting. C2C12 cells were transfected with vectors expressing different shRNAs against MuRF1 or a shScrambled (negative control) together with a vector encoding murine Flag-MuRF1. Oligos #461 were the most effective in knocking down MuRF1 protein levels. (**B**) RNAi-mediated knockdown of endogenous MuRF1 transcript levels in vivo quantified by qRT-PCR. *p<0.0.5, n=4 muscles.

7.2. Combinatorial knocking-down of MuRF1 and FoxO1/3 demonstrated both protective effects from tumor-induced muscle loss and hypertrophic effect on control mice

As an experimental plan, *in vivo* transfection experiments were conducted through intramuscular injection of expression plasmids (the selected shMuRF1 and/or shFoxO1/3 already available and previously tested in the lab) into the mice tibialis anterior muscle, followed by electroporation. At the same day, the subcutaneous inoculation of a C26 colon carcinoma cell suspension was administrated into the back of 7-week-old BALB/c mice in order to trigger cancer-induced cachexia, while the control group of mice received physiological PBS solution only. At the experimental endpoint, which occurred approximately 2 weeks after tumor implantation, as determined by ethical criteria (loss of ~25% of the initial body mass), electroporated muscles were collected and promptly frozen in liquid nitrogen (Figure 13).
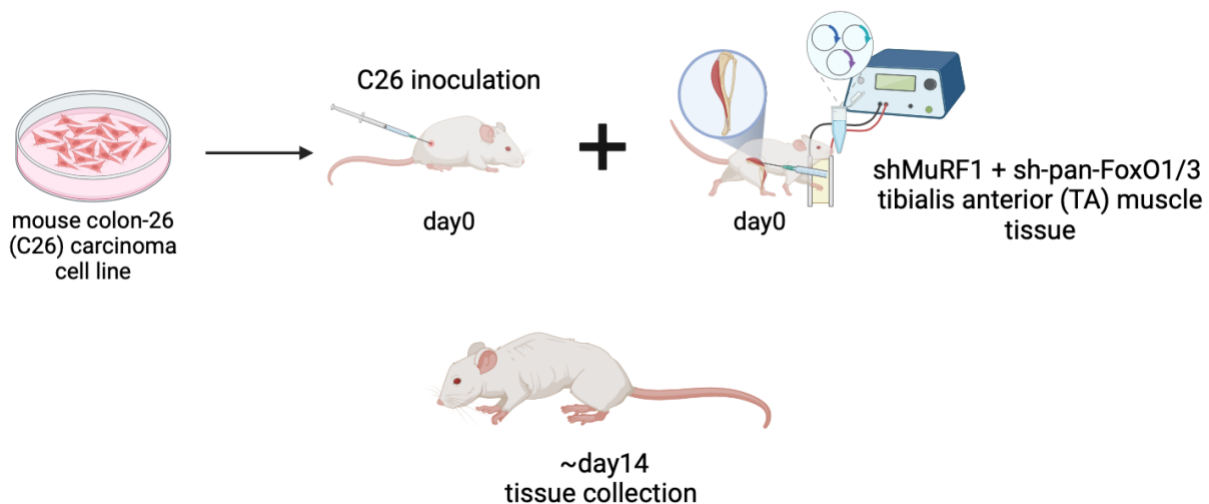

Figure 13: Experimental scheme

For cross-sectional area analysis, the transfected muscle fibers, identified by GFP fluorescence, and untransfected muscle fibers were subsequently measured. According to the results, when the cross-sectional area of muscle fibers was analyzed, we observed that knocking of FoxO1/3 led to a partial protection from muscle atrophy in the C26 tumor-bearing group, and knocking down of MuRF1 protected completely from tumor-induced muscle loss in the C26 group. Knocking down of FoxO1/3 and MuRF1 in combination prevented muscle loss in the tumor-bearing mice group. In the control group (basal condition), only the combinatorial knockdown of FoxO1/3 and MuRF1 resulted in increased muscle fiber cross-sectional area (Figure 14A-B).

Moreover, when the protective effect (% of control) of knocking down MuRF1 and FoxO1/3 was analyzed, we observed that shMuRF1 and shFoxO1/3 combinatorial administration accounts for higher protection from tumor-induced muscle loss than the single treatments alone (Figure 14B).

A
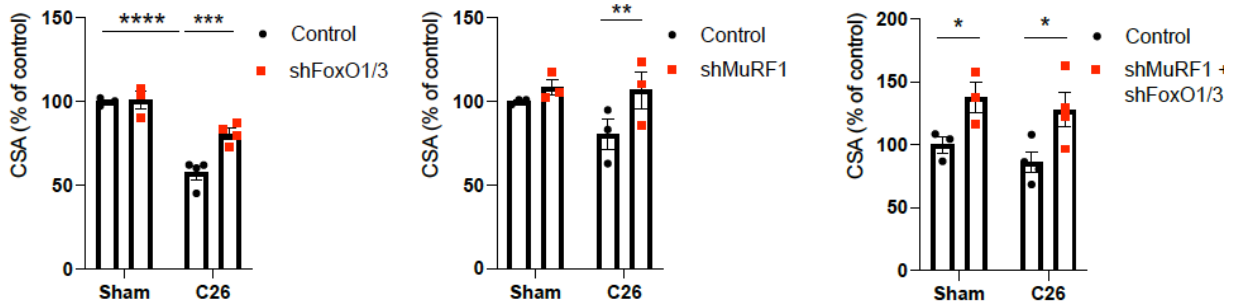
B
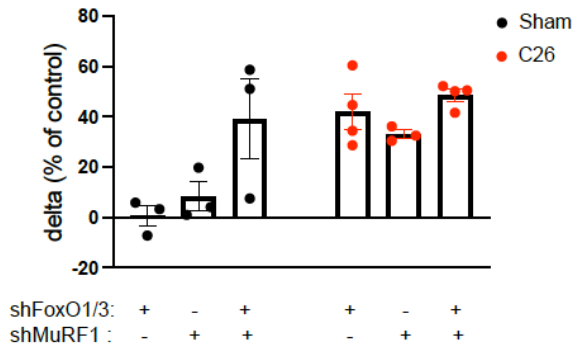
Figure 14: (A) Cross-sectional area (CSA) of GFP-positive TA muscle fibers transfected with co-cistronic expression plasmids encoding EmGFP, and shRNAs against FoxO1/3, MuRF1, and FoxO1/3 + MuRF1 compared to untransfected fibers (control) **(B)** difference (%) in size between transfected and untransfected fibers in control (Sham) and C26-bearing muscle. n=3/4 muscles. A two-way ANOVA with Benjamini, Krieger, and Yekutieli adjustment. $*p<0.0.5$, $**p<0.01$, $***p<0.001$, $****p<0.0001$

7.3. Setting up a Spatial Transcriptomics experiment aiming at deciphering the underlying gene and molecular profiles of shFoxO1/3 and shMuRF1 transfected muscle fibers in tumor-bearing mice

Our results (Figure 14A-B) suggest that targeting MuRF1 and FoxO1/3 in combination may play synergistic roles in the homeostatic control of skeletal muscle mass. To understand the underlying molecular pathways and discover the gene expression profiles in the comparison of control vs. C26 tumor-bearing vs. C26 tumor-bearing shFoxO1/3 and shMuRF1 transfected muscles' groups, we set up a spatial transcriptomics experiment.

We applied the experimental scheme described in Figure 15 to the three experimental groups (control, C26, C26 treated) in order to set up the spatial transcriptomic experiment. Indeed, we aim to discover and compare the transcriptome profile of muscles of control mice, cachectic mice, and cachectic mice which muscle-targeted inhibition of MuRF1 and FoxO1/3. First of all, we applied different fixation times (7h, 12h and 24h) in 10% Neutral Buffered Formalin of the collected tibialis anterior (TA) and extensor digitorium longus (EDL) muscles to reach our goal of preserving the morphological structure of the tissue sections and the integrity of the mRNA transcripts that are together necessary for optimal assay performance (Figure 16). As we can observe in Figure 16, on the left, from acquired H&E stained muscle sections pictures, 12h of fixation time (Figure 16B) was optimal in conserving muscle fiber structure and morphology. On the other hand, preserving RNA quality and integrity, evaluated by mean RNA fragments size, is the crucial step for library preparation for conducting spatial transcriptomics experiments. For this reason, this brings the necessity to have a measured percentage of total RNA fragments containing >200 nucleotides (DV200) (dotted line in Fig. 16), which is optimal assessed RNA quality for library preparation. According to these results, it has been decided to proceed with experiments with 12h fixation time (Figure 16B) since it is the right compromise in order to have preserved muscle morphology (for the spatial aspect) and RNA integrity (for the transcriptomics approach).
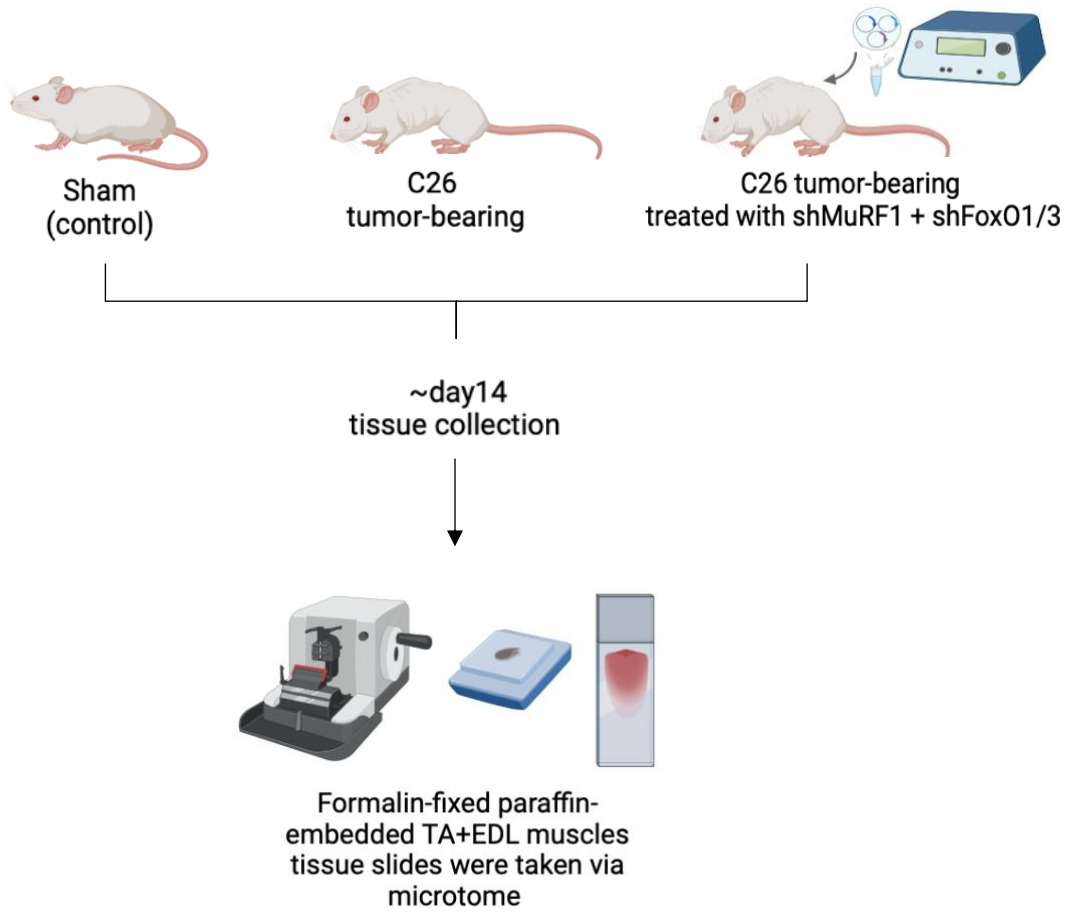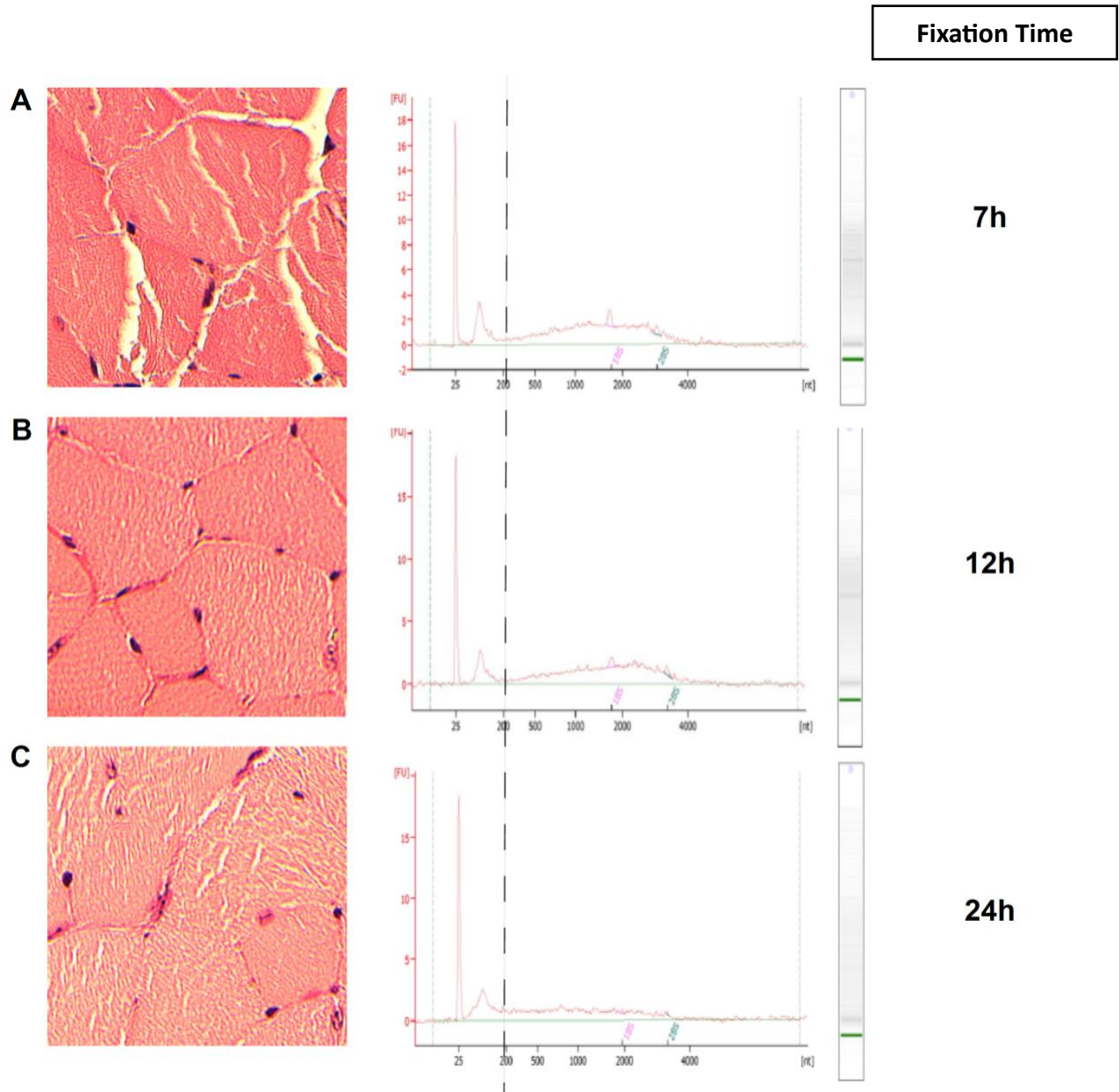
Figure 15: Experimental scheme

Figure 16: On the left, representative hematoxylin and eosin-stained (H&E) cryosections of TA muscles at different fixation times. On the right, bioanalyzer profile of RNA extracted from FFPE muscle slices at different fixation times **(A)** 7h of fixation, **(B)** 12h of fixation, **(C)** 24h of fixation in 10% Neutral Buffered Formalin.

Our ultimate goal with spatial transcriptomics is to characterize and compare the molecular signature of these three experimental groups in spatial location. Moreover, we aim at comparing the transcriptome of the C26 tumor-bearing mice's treated myofibers with the untreated ones. Therefore, we applied immunofluorescence (IF) protocol on formalin-fixed paraffin-embedded (FFPE) electroporated muscle cryosection slices with the goal of distinguishing the fibers transfected with our therapeutic co-cistronic plasmids encoding GFP from the untransfected ones. As shown in Figure 17, we were able to observe and discriminate the GFP-positive shMuRF1 and shFoxO1/3 transfected muscle fibers from the untransfected muscle fibers which are in the surroundings (Figure 17A-B).

Following these steps, muscle cryosection slices were sent to the genomic facility in order to be processed for the following experimental steps of the spatial transcriptomics protocol.
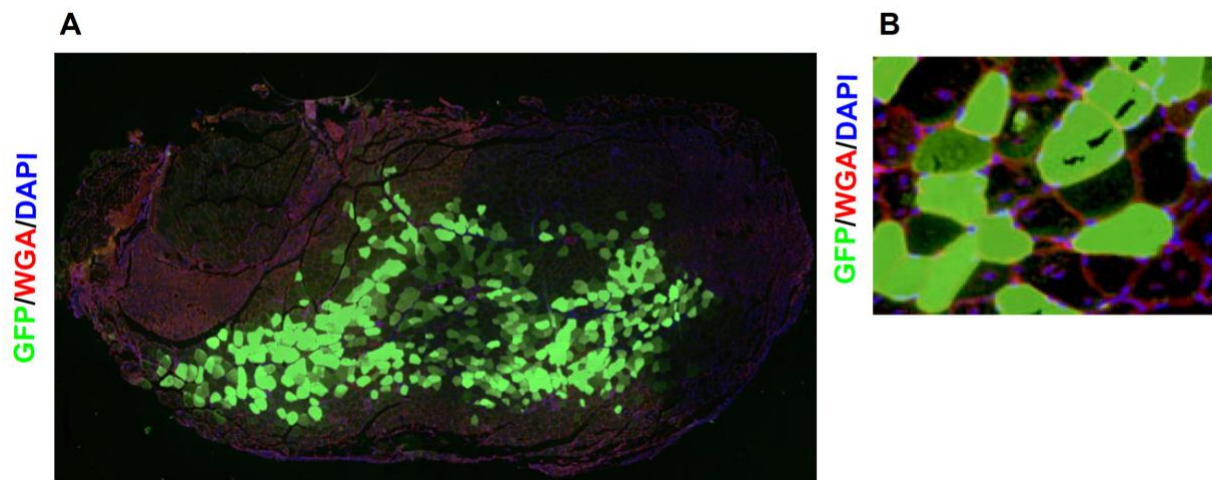

Figure 17: (A) Cryosections of FFPE TA + EDL muscles immunostained for GFP (in green), wheat germ agglutinin staining (red), 4',6-diamidino-2-phenylindole (blue). **(B)** A higher magnification image of the muscle fibers is shown in (A).

7.4. Raw data collection and preprocessing outputs of the spatial transcriptomics experiment

We proceed performing the spatial transcriptomic experiment, taking advantage of the Visium Spatial Gene Expression platform (10x Genomics).. The experiment was conducted on TA of sham, C26-tumor bearing mice and C26-tumor bearing mice, in which we transfected by electroporation the combination of shFoxO1/3 and shMuRF1 constructs. For each capture are on the slide, we managed to assemble 3 muscles (TA+EDL) for Sham condition, 2 muscles for C26 condition and three muscles (per 2 capture areas) for C26 treated with shFoxO1/3 and shMuRF1 constructs.

We then obtained initial output data of the spatial transcriptomics experiment. The analysis steps of spatial transcriptomics cover the preprocessing step of raw spatial transcriptomic data. It includes image correction and stitching, image registration, and assigning spatial context. Thereafter, the cell segmentation step allows the assignment of the reads to individual fibers based on spatial barcode and/or UMI (unique molecular identifiers) counting unique to each spatial spot (Dries et al., 2021). Spatial barcoding procedure is important in identifying RNA molecules which are coded to represent location via captured RNA molecules by single-molecule imaging. Within this, the located barcodes allow us to obtain information on captured RNA from the fibers tagged with spatial barcodes (Walker et al., 2022).

According to our obtained results outputs from data preprocessing, we acquired a summary file via Space Ranger analysis software for the Visium Spatial Gene Expression for FFPE library assay, which contains representative metrics. This can be used to assess the overall success of the experiment.

The criteria for evaluating the overall success of spatial transcriptomic experiment include these sequencing metrics: number of reads, valid barcodes, valid UMIs, sequencing saturation, Q30 bases in barcode, Q30 bases in probe read, and Q30 bases in UMI, umber of spots under tissue, mean reads per spot and median genes per spot.

As said above, in the spatial transcriptomic experiment setup, our ultimate goal was to compare the whole transcriptome profile of three experimental groups, control mice, cachectic mice, and cachectic mice treated with shMuRF1 and shFoxO1/3. Our representative summary files from preprocessing sequencing analysis of raw data (Figure 18A-D, Figure 19A-B) demonstrated that our experimental setup and library preparation worked successfully.

Initially, we evaluated the sequencing metrics of our preprocessing data output. The formalin-fixed-paraffin embedded (FFPE) tibialis anterior (TA) muscle tissue of control mice (Sham) (Figure 18A) resulted in 36.2% sequencing saturation, and 44.746.693 total number of read pairs.
The valid barcodes and the valid UMIs values should be higher than 75%, since lower values may indicate issues with sequencing or library quality. In our case of control mice, it is obtained 98% and 100%, respectively. The values of Q30 bases in barcode/UMI, and Q30 bases in probe read, which represents a fraction of tissue-associated barcode and the fraction of RNA read bases and associate with sequencing quality, correspond to our needs and desires with high base percentage numbers.
The FFPE TA muscle tissue of C26 tumor-induced cachectic mice (Figure 18B) resulted in the desired sequencing quality, with a high number of read pairs (34.111.393), 30.2% of sequencing saturation, and optimal values of other sequencing metrics parameters.
The FFPE TA muscle tissue of C26 tumor-induced cachectic mice locally treated by electroporation with shMuRF1 and shFoxO1/3 (Figure 18C-D) also resulted in optimal sequencing quality by covering all the factors of expected sequencing metrics values.

Secondly, according to the analysis of spots metrics, the FFPE TA muscle tissue of control mice (Sham) (Figure 18A) resulted in 1.393 fraction reads in spots under tissue. Moreover, the mean reads per tissue covered spot value is 32.123, which is higher than the minimum recommended. The median genes per spot value is 2.879, which represents the median number of genes detected per tissue-covered spot, and this detection is defined as the presence of at least one UMI count.

The spot metrics values of both FFPE TA muscle tissue from C26 tumor-induced cachectic mice (Figure 18B) and FFPE cachectic muscle tissue treated with shMuRF1 and shFoxO1/3 (Figure 18C-D) represented the desired acquisition of number of read spots under the tissue, mean reads, and mean genes per spot and, importantly, all the metrics were comparable between the different experimental groups (Figure 18A-D).

A)

B) ## Sample_S54410_C26Ctrl_7_9_11

Summary | Gene Expression

1,169
Number of Spots Under Tissue

29,180
Mean Reads per Spot

2,942
Median Genes per Spot

Sequencing ⓘ

Number of Reads	34,111,393
Valid Barcodes	98.2%
Valid UMIs	100.0%
Sequencing Saturation	30.2%
Q30 Bases in Barcode	96.4%
Q30 Bases in Probe Read	97.0%
Q30 Bases in UMI	96.2%

Image ⓘ

Tissue Detection and Fiducial Alignment

C) ## Sample_S54408_C26Sh_17_19_21

Summary | Gene Expression

1,393
Number of Spots Under Tissue

30,170
Mean Reads per Spot

3,519
Median Genes per Spot
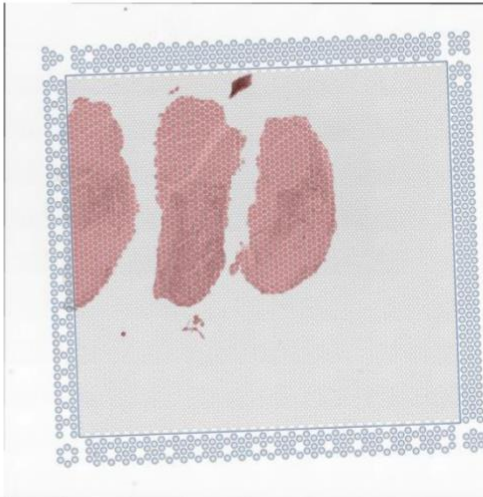
Sequencing ⓘ

Number of Reads	42,026,257
Valid Barcodes	98.4%
Valid UMIs	100.0%
Sequencing Saturation	25.9%
Q30 Bases in Barcode	96.4%
Q30 Bases in Probe Read	97.3%
Q30 Bases in UMI	96.2%

Image ⓘ

Tissue Detection and Fiducial Alignment

D) Sample_S54409_C26Sh_16_18_20

Summary | Gene Expression

1,239
Number of Spots Under Tissue

29,036
Mean Reads per Spot

3,671
Median Genes per Spot

Sequencing

Number of Reads	35,975,380
Valid Barcodes	98.3%
Valid UMIs	100.0%
Sequencing Saturation	23.2%
Q30 Bases in Barcode	96.4%
Q30 Bases in Probe Read	97.1%
Q30 Bases in UMI	96.3%

Image
Tissue Detection and Fiducial Alignment
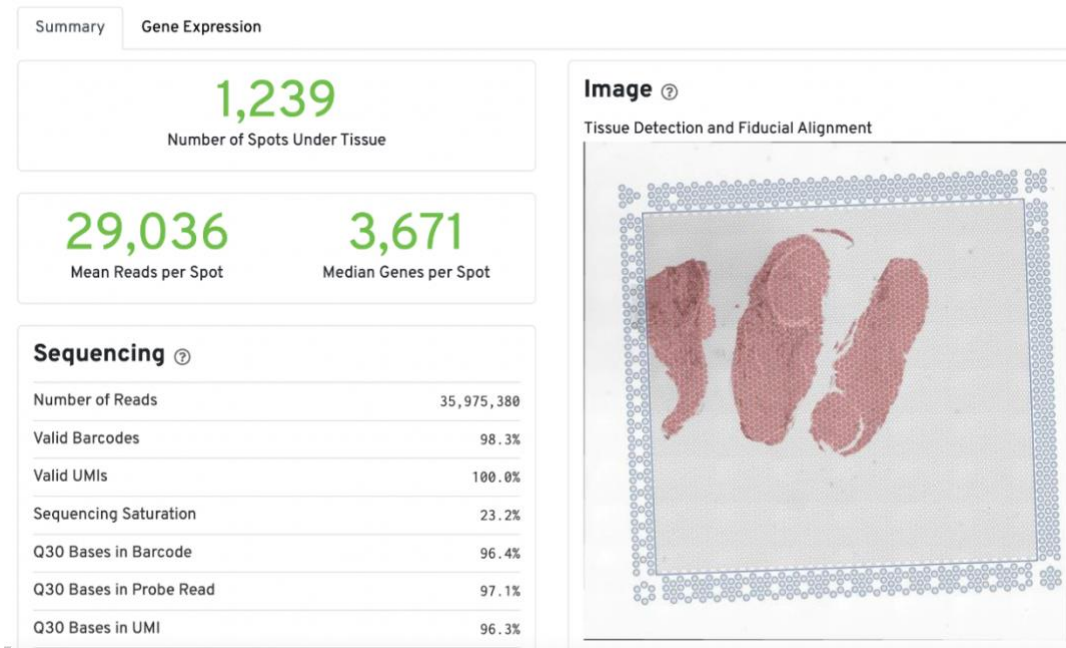
Figure 18A-D: The tables represent the preprocessing of raw microscopic imaging-based spatial transcriptomics data. The reads, barcode/UMI counts, detected spots, and genes per spot constitute pre-processing yields for subsequent downstream analyses of spatial transcriptomics. These reported values are provided via the SpaceRanger tool 10x Visium Spatial Gene Expression for FFPE assay. **A)** refers to the information on TA + EDL muscle tissues of Sham (control) mice (n=3). **B)** refers to the information on TA + EDL muscle tissues of C26-tumor-bearing mice (n=2). **C) & D)** refer to the information on TA + EDL muscle tissues of electroporated GFP-embedded shMuRF1 + shFoxO1/3 in C26-tumor bearing mice (n=6).

Furthermore, we can observe the output data of captured imaging and spatially segmented regions of single muscle fibers of cachectic FFPE TA muscles treated with shMuRF1 and shFoxO1/3 (Figure 19A-B).

Cell segmentation allows us to locate and decode individual spots on tissue, corresponding to single gene transcripts, thus enable us to understand spatial distribution of gene expression within the tissue sample. (Dries et al., 2021). This step also allows us to identify different clustered cell types on muscle tissue and their quantification. Subsequent analysis yields a transcriptomics profile of three experimental groups (Sham, C26, C26 + shMuRF1 & shFoxO1/3) identifying expression patterns based on spatial coordinates.

A) 17_19_21

B) 16_18_20
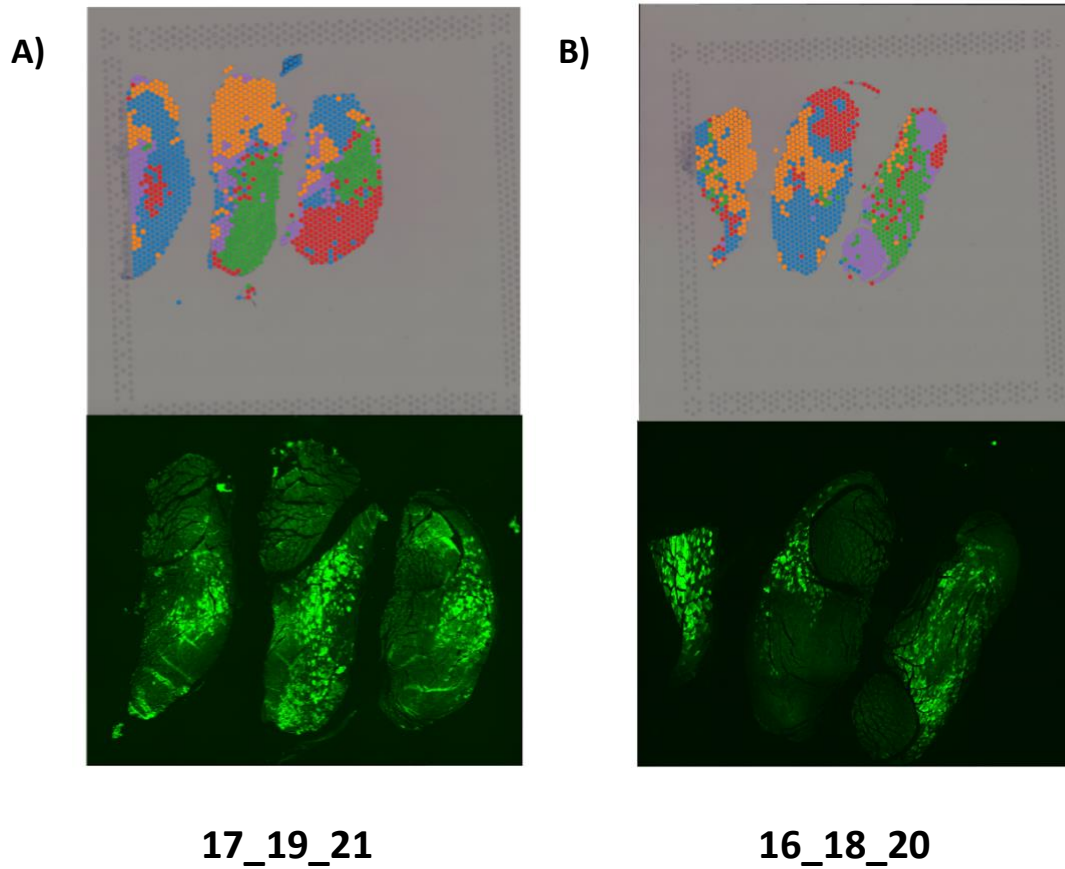
Figure 19A-B: The figure represents spatially resolved transcriptomics data that highlights discrete anatomical units characterized by different transcriptionally identified cell types. **A) & B)** represents section of TA + EDL muscle tissues electroporated with GFP-embedded shMuRF1 and shFoxO1/3 (n=6) from tumor-bearing mice. Visium array spots are color-coded based on cluster assignment, and clustered colors indicate different cell types.

8. Discussion

The characteristics of cancer cachexia (CC) consist of weight loss, muscle atrophy, weakness, fat reduction, and systemic inflammation. Cachexia occurs in 70%-80% of advanced cancer patients and constitutes up to 30% of cancer-associated deaths. It is highly correlated with cancers involving the pancreas, lungs, stomach, and liver which and. Indeed, cancer cachexia development is dependent on tumor type, and the prevalence in gastric/pancreatic cancer patients is ~80%, in lung/colon cancer patients is ~50%, and in breast cancer patients is ~40% (Ahmad et al., 2022; Park et al., 2023). However, the severity and/or the development of cancer-associated cachexia is often not related to tumor size or stage, and relatively small size tumors can lead to severe wasting (Petruzzelli & Wagner, 2016).

A crucial problem of this syndrome is the lack of an effective therapy: although in clinical practice a multimodal approach, that comprises nutritional therapy, administration of appetite-modulating drugs (ghrelin above all), anti-inflammatory interventions and/or exercise therapy, has been already adopted, cachexia remains an unsolved problem to most cancer patients.

In cancer-induced cachexia, the loss of skeletal muscle is specifically problematic and clinically relevant for patients causing profound weakness and decreasing their quality of life. In addition, skeletal muscle loss leads to decreased tolerance to anti-cancer treatment and survival in those patients (Talbert & Guttridge, 2016).
Indeed, studies on cancer cachexia both in human cancer patients and different cancer-induced cachectic animal models reported increased skeletal muscle loss compared to control groups (Martin & Freyssenet, 2021) and counteracting skeletal muscle wasting in cancer cachexia preclinical models prolongs survival independently on tumor growth (X. Zhou et al., 2010a)
The loss of skeletal muscle in cancer patients is one of the results associated with tumor-related altered whole-body metabolism. The synergistic action of many altered signaling pathways and

inflammatory cytokines play a key role in leading to muscle atrophy and altered muscle metabolism in cachexia.

One of the main mechanisms leading to muscle atrophy is the unbalancing between protein synthesis and degradation: decreased protein synthesis and increased protein degradation cause decreases in muscle fiber cross-sectional area (Talbert & Guttridge, 2016). Protein degradation is mostly mediated by the two major proteolytic systems in the cells: the ubiquitin-proteasome and autophagy-lysosome protein degradation systems (Sartori, Romanello, et al., 2021a).

These two processes are tightly regulated and are under the control of a precise transcriptional program. Gene expression profiling studies revealed that in different catabolic condition characterized by muscle atrophy, including cancer cachexia, there is a subset of genes that are commonly up- or down-regulated in the muscles. For this reason, they were called *Atrogens.* The two most induced genes were two muscle specific E3 ubiquitin ligases, *Atrogin-1/MAFBx and MuRF1* required to initiate and maintain an atrophy program (Lecker et al., 2004; Sacheck, Hyatt, Raffaello, Thomas Jagoe, et al., 2007). Indeed, it has been demonstrated that the muscle-specific deletion of Atrogin-1/MAFbx or Murf1 (muscle RING finger protein 1) resulted in a protective effect on skeletal muscle from experimental atrophy (Bodine et al., 2001a).

These atrophy-related ubiquitin ligases involved in protein breakdown are under the negative control of the IGF/Akt pathway a growth-promoting pathway that not only induces protein synthesis but also inhibits protein degradation by blocking the transcription activity of FoxOs that have a crucial role in the upregulation of Atrogin-1 and MuRF-1 in muscle atrophy (Bollinger et al., 2014; Sandri et al., 2004; Waddell et al., 2008).

However, MuRF1 is also under the control of other FoxOs-independent inflammatory signaling pathways such as TNF-α/NFkβ and TWEAK ones, that are highly induced in cancer cachexia (Adams et al., 2020; Webster et al., 2020).

Indeed, the research which has been conducted on tumor-bearing mice demonstrated that inhibiting FoxO proteins (FoxO1/3/4) prevented tumor-induced muscle loss in mice and downregulated transcriptional activities of Atrogin-1 and MuRF1 (Judge et al., 2014; Reed et al., 2012). In another study, it was observed that targeted knockdown of FoxP1, FoxO1-dependent protein, via shRNA in C26 tumor-bearing mice resulted in partial protection from cancer-induced muscle loss (Neyroud et al., 2021). In another recent study which has been conducted on MuRF1 activity in pancreatic tumor-bearing mice, it is observed that deletion of MuRF1 protected tumor-induced muscle and fat wasting, slowed tumor growth, and extended survival (Neyroud et al., 2023).

Although many studies have focused on inhibition/deletion of key atrophic markers such as *Atrogin1* and *FoxOs* to prevent muscle atrophy in cancer cachexia (Liu et al., 2007), regulating and silencing the expression of gene/s of interest via RNAi-based approach still hold up its novelty (Zhu et al., n.d.).

For this reason, our work aims to counteract skeletal muscle wasting in cancer cachexia by developing RNAi-based therapeutics targeting the expression of *FoxO1/3* and *MuRF1* alone or in combination. This approach provides us with more precision therapy for cancer-induced cachexia.

According to our experimental goal, we conducted the RNAi-based knockdown experiment targeting FoxO1/3 and MurF1 in C26 tumor-induced mice. From our results, we observed that knocking down of FoxO1/3 resulted in partial protection of tumor-induced skeletal muscle wasting. On the contrary, knocking down of MuRF1 in tumor-bearing mice rescued tumor-mediated skeletal muscle loss.

Intriguingly, when we applied a combinatorial knockdown by co-transfecting both shFoxO1/3 and shMuRF1 in the muscles of tumor-bearing mice, we observed not only complete protection of tumor-induced muscle loss in C26 mice but also a hypertrophic effect on control mice. Indeed, this approach was sufficient to increase muscle fiber cross-sectional area in basal condition.

Moreover, the protective effect (% of control) of knocking down both MuRF1 and FoxO1/3 resulted in a higher trend than the protective effect of the single treatments alone.

These experimental results suggest that RNAi targeting could be a successful therapeutic approach due to its ability to silence multiple target genes simultaneously (Lambeth & Smith, 2013). Specifically, the targeted delivery of RNAi constructs against a combination of different targets specifically to the skeletal muscle could not only be a promising way to rescue skeletal muscle wasting in cancer-associated cachexia but also prevent muscle atrophy in other pathological conditions.

These data also suggested us that there may be synergistic roles between MuRF1 and FoxO1/3. Therefore, to understand better the involved underlying molecular pathways, we set up a spatial transcriptomics experiment, comparing the muscle tissues of control, cachectic, and cachectic mice treated with shMuRF1 and shFoxO1/3. This -omics approach allows us to profile the gene activity and map where it is occurring in cachectic muscles compared to control in spatial location, and to understand if and how the cachectic signature is reversed by the combined therapeutic approach.

To conduct spatial transcriptomics analyses, we fixed the dissected TA and EDL muscle tissues with formalin. By selecting the optimal fixation time from our different time-point trials, we were able to both preserve RNA integrity and muscle fibers' morphological structures, which would have been necessary for continuing spatial transcriptomics analysis. In addition, we aim to discriminate shMurF1 + shFoxO1/3 transfected muscle fibers from untransfected ones in tumor-bearing cancer cachectic mice muscle tissues in order to compare and decipher transcriptome activity. Since our plasmids encode shRNAs and GFP, we were able to discriminate targeted GFP positive muscle fibers by immunofluorescence staining on FFPE muscle tissues.

According to our experimental results, our preliminary preprocessing data outputs from spatial transcriptomics analysis gave us read spots, gene spots, barcode/UMI counting, and cell segmentation profiles in order to assign reads to individual anatomical areas covering each spot. These results demonstrated that we were able to set up and perform all the necessary steps from

the experimental point of view. With further steps of spatial transcriptomics analyses, we will be able to acquire spatially located whole transcriptome activity profiles, and gene expression patterns of different muscle's anatomical regions and subpopulations in three groups (sham, C26, C26 + shMuRF1 & shFoxO1/3).

In conclusion, it is known that many signaling pathways and gene regulatory networks are involved in muscle wasting in cancer-induced cachexia. Our work demonstrated that the combinatorial knockdown approach could be a key in precision medicine of muscle wasting in cancer cachexia due to its ability to target multiple genes simultaneously. Spatial transcriptomics analyses will allow us to understand atrophic muscle tissue composition in the cancer-induced cachectic state by deciphering the underlying gene expression profiles, biomarker identification, and spatial composition of cells/nuclei within the tissue.

Our future endeavors will focus on 1) designing shRNA oligos for targeting other molecular players/combination of players involved in cancer-induced muscle atrophy with the implementation of systemic delivery of shRNAs with adeno-associated viruses (AAV) vectors to target all muscles within the body; 2) generating human shRNA oligos and testing them into cachectic neuromuscular organoids derived from human iPSC to prove the translatability of our preclinical results.

These approaches can broaden the horizon of precision and personalized medicine for combating skeletal muscle wasting in cancer cachexia via RNAi-based therapy.

9. References

Adams, V., Gußen, V., Zozulya, S., Cruz, A., Moriscot, A., Linke, A., & Labeit, S. (2020). Small-Molecule Chemical Knockdown of MuRF1 in Melanoma Bearing Mice Attenuates Tumor Cachexia Associated Myopathy. *Cells*, *9*(10). https://doi.org/10.3390/CELLS9102272

Ahmad, S. S., Ahmad, K., Shaikh, S., You, H. J., Lee, E. Y., Ali, S., Lee, E. J., & Choi, I. (2022). Molecular Mechanisms and Current Treatment Options for Cancer Cachexia. *Cancers*, *14*(9). https://doi.org/10.3390/CANCERS14092107

Aversa, Z., Costelli, P., & Muscaritoli, M. (2017). Cancer-induced muscle wasting: Latest findings in prevention and treatment. In *Therapeutic Advances in Medical Oncology* (Vol. 9, Issue 5, pp. 369–382). SAGE Publications Inc. https://doi.org/10.1177/1758834017698643

Baracos, V. E., Martin, L., Korc, M., Guttridge, D. C., & Fearon, K. C. H. (2018). Cancer-associated cachexia. *Nature Reviews Disease Primers*, *4*, 1–18. https://doi.org/10.1038/nrdp.2017.105

Bechet, D., Tassa, A., Taillandier, D., Combaret, L., & Attaix, D. (2005). Lysosomal proteolysis in skeletal muscle. *International Journal of Biochemistry and Cell Biology*, *37*(10 SPEC. ISS.), 2098–2114. https://doi.org/10.1016/j.biocel.2005.02.029

Bodine, S. C., & Baehr, L. M. (2014a). Skeletal muscle atrophy and the E3 ubiquitin ligases MuRF1 and MAFbx/atrogin-1. *American Journal of Physiology - Endocrinology and Metabolism*, *307*(6), E469. https://doi.org/10.1152/AJPENDO.00204.2014

Bodine, S. C., Latres, E., Baumhueter, S., Lai, V. K., Nunez, L., Clarke, B. A., Poueymirou, W. T., Panaro, F. J., Na, E., Dharmarajan, K., Pan, Z. Q., Valenzuela, D. M., DeChiara, T. M., Stitt, T. N., Yancopoulos, G. D., & Glass, D. J. (2001). Identification of ubiquitin ligases required for skeletal muscle atrophy. *Science (New York, N.Y.)*, *294*(5547), 1704–1708. https://doi.org/10.1126/science.1065874

Bollinger, L. M., Witczak, C. A., Houmard, J. A., & Brault, J. J. (2014). SMAD3 augments FoxO3-induced MuRF-1 promoter activity in a DNA-binding-dependent manner. *American Journal of Physiology - Cell Physiology*, *307*(3), 278–287.

https://doi.org/10.1152/AJPCELL.00391.2013/ASSET/IMAGES/LARGE/ZH00151475600006.J
PEG

Bonaldo, P., & Sandri, M. (2013). Cellular and molecular mechanisms of muscle atrophy. *Disease Models & Mechanisms*, *6*(1), 25–39. https://doi.org/10.1242/dmm.010389

Bonetto, A., Aydogdu, T., Jin, X., Zhang, Z., Zhan, R., Puzis, L., Koniaris, L. G., & Zimmers, T. A. (2012). JAK/STAT3 pathway inhibition blocks skeletal muscle wasting downstream of IL-6 and in experimental cancer cachexia. *Am J Physiol Endocrinol Metab*, *303*, 410–421. https://doi.org/10.1152/ajpendo.00039.2012.-Cachexia

Bonetto, A., Aydogdu, T., Kunzevitzky, N., Guttridge, D. C., Khuri, S., Koniaris, L. G., & Zimmers, T. A. (2011). STAT3 Activation in Skeletal Muscle Links Muscle Wasting and the Acute Phase Response in Cancer Cachexia. *PLOS ONE*, *6*(7), e22538. https://doi.org/10.1371/JOURNAL.PONE.0022538

Bottinelli, R., & Reggiani, C. (2000). Human skeletal muscle fibres: Molecular and functional diversity. *Progress in Biophysics and Molecular Biology*, *73*(2–4), 195–262. https://doi.org/10.1016/S0079-6107(00)00006-7

Bozzetti, F., & Mariani, L. (2009). Defining and classifying cancer cachexia: a proposal by the SCRINIO Working Group. *JPEN. Journal of Parenteral and Enteral Nutrition*, *33*(4), 361–367. https://doi.org/10.1177/0148607108325076

Cai, D., Frantz, J. D., Tawa, N. E., Melendez, P. A., Oh, B. C., Lidov, H. G. W., Hasselgren, P. O., Frontera, W. R., Lee, J., Glass, D. J., & Shoelson, S. E. (2004). IKKβ/NF-κB Activation Causes Severe Muscle Wasting in Mice. *Cell*, *119*(2), 285–298. https://doi.org/10.1016/J.CELL.2004.09.027

Clavel, S., Siffroi-Fernandez, S., Coldefy, A. S., Boulukos, K., Pisani, D. F., & Dérijard, B. (2010). Regulation of the Intracellular Localization of Foxo3a by Stress-Activated Protein Kinase Signaling Pathways in Skeletal Muscle Cells. *Molecular and Cellular Biology*, *30*(2), 470. https://doi.org/10.1128/MCB.00666-09

da Fonseca, G. W. P., Farkas, J., Dora, E., von Haehling, S., & Lainscak, M. (2020). Cancer Cachexia and Related Metabolic Dysfunction. *International Journal of Molecular Sciences*, *21*(7). https://doi.org/10.3390/IJMS21072321

Dalal, S. (2019). Lipid metabolism in cancer cachexia. *Annals of Palliative Medicine*, *8*(1), 133–123. https://doi.org/10.21037/APM.2018.10.01

Dries, R., Chen, J., Del Rossi, N., Khan, M. M., Sistig, A., & Yuan, G. C. (2021). Advances in spatial transcriptomic data analysis. *Genome Research*, *31*(10), 1706. https://doi.org/10.1101/GR.275224.121

Ebrahimi, B., Tucker, S. L., Li, D., Abbruzzese, J. L., & Kurzrock, R. (2004). Cytokines in pancreatic carcinoma: correlation with phenotypic characteristics and prognosis. *Cancer*, *101*(12), 2727–2736. https://doi.org/10.1002/CNCR.20672

Fanzani, A., Conraads, V. M., Penna, F., & Martinet, W. (2012). Molecular and cellular mechanisms of skeletal muscle atrophy: an update. *Journal of Cachexia, Sarcopenia and Muscle*, *3*(3), 163. https://doi.org/10.1007/S13539-012-0074-6

Fearon, K. C. H., Glass, D. J., & Guttridge, D. C. (2012). Cancer cachexia: Mediators, signaling, and metabolic pathways. In *Cell Metabolism* (Vol. 16, Issue 2, pp. 153–166). https://doi.org/10.1016/j.cmet.2012.06.011

Fearon, K., Strasser, F., Anker, S. D., Bosaeus, I., Bruera, E., Fainsinger, R. L., Jatoi, A., Loprinzi, C., MacDonald, N., Mantovani, G., Davis, M., Muscaritoli, M., Ottery, F., Radbruch, L., Ravasco, P., Walsh, D., Wilcock, A., Kaasa, S., & Baracos, V. E. (2011). Definition and classification of cancer cachexia: An international consensus. *The Lancet Oncology*, *12*(5), 489–495. https://doi.org/10.1016/S1470-2045(10)70218-7

Fernandes, T., Soci, Ú. P. R., Melo, S. F. S., Alves, C. R., Oliveira, E. M., Fernandes, T., Soci, Ú. P. R., Melo, S. F. S., Alves, C. R., & Oliveira, E. M. (2012). Signaling Pathways that Mediate Skeletal Muscle Hypertrophy: Effects of Exercise Training. *Skeletal Muscle - From Myogenesis to Clinical Relations*. https://doi.org/10.5772/51087

Flück, M., & Hoppeler, H. (2003). Molecular basis of skeletal muscle plasticity--from gene to form and function. *Reviews of Physiology, Biochemistry and Pharmacology*, *146*, 159–216. https://doi.org/10.1007/S10254-002-0004-7

Frontera, W. R., & Ochala, J. (2015). Skeletal Muscle: A Brief Review of Structure and Function. *Behavior Genetics*, *45*(2), 183–195. https://doi.org/10.1007/s00223-014-9915-y

Fry, C. S., Nayeem, S. Z., Dillon, E. L., Sarkar, P. S., Tumurbaatar, B., Urban, R. J., Wright, T. J., Sheffield-Moore, M., Tilton, R. G., & Choudhary, S. (2016). Glucocorticoids increase skeletal muscle NF-κB inducing kinase (NIK): links to muscle atrophy. *Physiological Reports*, *4*(21). https://doi.org/10.14814/PHY2.13014

Geremia, A., Sartori, R., Baraldo, M., Nogara, L., Balmaceda, V., Dumitras, G. A., Ciciliot, S., Scalabrin, M., Nolte, H., & Blaauw, B. (2022). Activation of Akt–mTORC1 signalling reverts cancer-dependent muscle wasting. *Journal of Cachexia, Sarcopenia and Muscle*, *13*(1), 648. https://doi.org/10.1002/JCSM.12854

Gillies, A. R., & Lieber, R. L. (2011). Structure and function of the skeletal muscle extracellular matrix. *Muscle and Nerve*, *44*(3), 318–331. https://doi.org/10.1002/mus.22094

Gilmore, L. A., Parry, T. L., Thomas, G. A., & Khamoui, A. V. (2023). Skeletal muscle omics signatures in cancer cachexia: perspectives and opportunities. *JNCI Monographs*, *2023*(61), 30–42. https://doi.org/10.1093/JNCIMONOGRAPHS/LGAD006

Goodman, C. A., McNally, R. M., Hoffmann, F. M., & Hornberger, T. A. (2013). Smad3 Induces Atrogin-1, Inhibits mTOR and Protein Synthesis, and Promotes Muscle Atrophy In Vivo. *Molecular Endocrinology*, *27*(11), 1946. https://doi.org/10.1210/ME.2013-1194

Han, J., Meng, Q., Shen, L., & Wu, G. (2018). Interleukin-6 induces fat loss in cancer cachexia by promoting white adipose tissue lipolysis and browning. *Lipids in Health and Disease*, *17*(1). https://doi.org/10.1186/S12944-018-0657-0

Huang, B., Lang, X., & Li, X. (2022). *The role of IL-6/JAK2/STAT3 signaling pathway in cancers*. https://doi.org/10.3389/fonc.2022.1023177

Jaiswal, N., Gavin, M. G., Quinn, W. J., Luongo, T. S., Gelfer, R. G., Baur, J. A., & Titchenell, P. M. (2019). The role of skeletal muscle Akt in the regulation of muscle mass and glucose homeostasis. *Molecular Metabolism*, *28*, 1–13. https://doi.org/10.1016/J.MOLMET.2019.08.001

Johnston, A. J., Murphy, K. T., Jenkinson, L., Laine, D., Emmrich, K., Faou, P., Weston, R., Jayatilleke, K. M., Schloegel, J., Talbo, G., Casey, J. L., Levina, V., Wong, W. W. L., Dillon, H., Sahay, T., Hoogenraad, J., Anderton, H., Hall, C., Schneider, P., … Hoogenraad, N. J. (2015). Targeting of

Fn14 Prevents Cancer-Induced Cachexia and Prolongs Survival. *Cell*, *162*(6), 1365–1378. https://doi.org/10.1016/J.CELL.2015.08.031

Judge, S. M., Wu, C. L., Beharry, A. W., Roberts, B. M., Ferreira, L. F., Kandarian, S. C., & Judge, A. R. (2014). Genome-wide identification of FoxO-dependent gene networks in skeletal muscle during C26 cancer cachexia. *BMC Cancer*, *14*(1). https://doi.org/10.1186/1471-2407-14-997

Kadakia, K. C., Hamilton-Reeves, J. M., & Baracos, V. E. (2023). Current Therapeutic Targets in Cancer Cachexia: A Pathophysiologic Approach. *American Society of Clinical Oncology Educational Book. American Society of Clinical Oncology. Annual Meeting*, *43*(43), e389942. https://doi.org/10.1200/EDBK_389942

Kamei, Y., Miura, S., Suzuki, M., Kai, Y., Mizukami, J., Taniguchi, T., Mochida, K., Hata, T., Matsuda, J., Aburatani, H., Nishino, I., & Ezaki, O. (2004). Skeletal muscle FOXO1 (FKHR) transgenic mice have less skeletal muscle mass, down-regulated Type I (slow twitch/red muscle) fiber genes, and impaired glycemic control. *The Journal of Biological Chemistry*, *279*(39), 41114–41123. https://doi.org/10.1074/JBC.M400674200

Kasprzak, A. (2021). The Role of Tumor Microenvironment Cells in Colorectal Cancer (CRC) Cachexia. *International Journal of Molecular Sciences*, *22*(4), 1–34. https://doi.org/10.3390/IJMS22041565

Kir, S., White, J. P., Kleiner, S., Kazak, L., Cohen, P., Baracos, V. E., & Spiegelman, B. M. (2014). Tumor-derived PTHrP Triggers Adipose Tissue Browning and Cancer Cachexia. *Nature*, *513*(7516), 100. https://doi.org/10.1038/NATURE13528

Kjær, M. (2004). Role of extracellular matrix in adaptation of tendon and skeletal muscle to mechanical loading. *Physiological Reviews*, *84*(2), 649–698. https://doi.org/10.1152/PHYSREV.00031.2003

Kollias, H. D., & McDermott, J. C. (2008). Transforming growth factor-β and myostatin signaling in skeletal muscle. *Journal of Applied Physiology*, *104*(3), 579–587. https://doi.org/10.1152/JAPPLPHYSIOL.01091.2007/ASSET/IMAGES/LARGE/ZDG0020877020003.JPEG

Lambeth, L. S., & Smith, C. A. (2013). Short hairpin RNA-mediated gene silencing. *Methods in Molecular Biology (Clifton, N.J.)*, *942*, 205–232. https://doi.org/10.1007/978-1-62703-119-6_12

Lecker, S. H., Goldberg, A. L., & Mitch, W. E. (2006). Protein Degradation by the Ubiquitin–Proteasome Pathway in Normal and Disease States. *Journal of the American Society of Nephrology*, *17*(7).

Lee, S. J., & McPherron, A. C. (2001). Regulation of myostatin activity and muscle growth. *Proceedings of the National Academy of Sciences of the United States of America*, *98*(16), 9306–9311. https://doi.org/10.1073/PNAS.151270098

Li, H.-H., Willis, M. S., Lockyer, P., Miller, N., Mcdonough, H., Glass, D. J., & Patterson, C. (2007). Atrogin-1 inhibits Akt-dependent cardiac hypertrophy in mice via ubiquitin-dependent coactivation of Forkhead proteins. *The Journal of Clinical Investigation*, *117*. https://doi.org/10.1172/JCI31757

Liu, C. M., Yang, Z., Liu, C. W., Wang, R., Tien, P., Dale, R., & Sun, L. Q. (2007). Effect of RNA oligonucleotide targeting Foxo-1 on muscle growth in normal and cancer cachexia mice. *Cancer Gene Therapy*, *14*(12), 945–952. https://doi.org/10.1038/SJ.CGT.7701091

Loumaye, A., De Barsy, M., Nachit, M., Lause, P., Frateur, L., Van Maanen, A., Trefois, P., Gruson, D., & Thissen, J. P. (2015). Role of Activin A and myostatin in human cancer cachexia. *The Journal of Clinical Endocrinology and Metabolism*, *100*(5), 2030–2038. https://doi.org/10.1210/JC.2014-4318

Malla, J., Zahra, A., Venugopal, S., Selvamani, T. Y., Shoukrie, S. I., Selvaraj, R., Dhanoa, R. K., Hamouda, R. K., & Mostafa, J. (2022). What Role Do Inflammatory Cytokines Play in Cancer Cachexia? *Cureus*, *14*(7). https://doi.org/10.7759/CUREUS.26798

Martin, A., & Freyssenet, D. (2021). Phenotypic features of cancer cachexia-related loss of skeletal muscle mass and function: lessons from human and animal studies. *Journal of Cachexia, Sarcopenia and Muscle*, *12*(2), 252–273. https://doi.org/10.1002/JCSM.12678

Masiero, E., Agatea, L., Mammucari, C., Blaauw, B., Loro, E., Komatsu, M., Metzger, D., Reggiani, C., Schiaffino, S., & Sandri, M. (2009). Autophagy is required to maintain muscle mass. *Cell Metabolism*, *10*(6), 507–515. https://doi.org/10.1016/j.cmet.2009.10.008

Miyazaki, M., & Esser, K. A. (2009). Regulation of Protein Metabolism in Exercise and Recovery: Cellular mechanisms regulating protein synthesis and skeletal muscle hypertrophy in animals. *Journal of Applied Physiology*, *106*(4), 1367. https://doi.org/10.1152/JAPPLPHYSIOL.91355.2008

Mueller, T. C., Bachmann, J., Prokopchuk, O., Friess, H., & Martignoni, M. E. (2016). Molecular pathways leading to loss of skeletal muscle mass in cancer cachexia – can findings from animal models be translated to humans? *BMC Cancer*, *16*(1). https://doi.org/10.1186/S12885-016-2121-8

Mukund, K., & Subramaniam, S. (2020a). Skeletal muscle: A review of molecular structure and function, in health and disease. *Wiley Interdisciplinary Reviews: Systems Biology and Medicine*, *12*(1), 1–46. https://doi.org/10.1002/wsbm.1462

Neyroud, D., Laitano, O., Dasgupta, A., Lopez, C., Schmitt, R. E., Schneider, J. Z., Hammers, D. W., Sweeney, H. L., Walter, G. A., Doles, J., Judge, S. M., & Judge, A. R. (2023). Blocking muscle wasting via deletion of the muscle-specific E3 ligase MuRF1 impedes pancreatic tumor growth. *Communications Biology 2023 6:1*, *6*(1), 1–17. https://doi.org/10.1038/s42003-023-04902-2

Neyroud, D., Nosacka, R. L., Callaway, C. S., Trevino, J. G., Hu, H., Judge, S. M., & Judge, A. R. (2021). FoxP1 is a transcriptional repressor associated with cancer cachexia that induces skeletal muscle wasting and weakness. *Journal of Cachexia, Sarcopenia and Muscle*, *12*(2), 421–442. https://doi.org/10.1002/JCSM.12666

Ni, J., & Zhang, L. (2020a). Cancer Cachexia: Definition, Staging, and Emerging Treatments. *Cancer Management and Research*, *12*, 5597. https://doi.org/10.2147/CMAR.S261585

Oliff, A., Defeo-Jones, D., Boyer, M., Martinez, D., Kiefer, D., Vuocolo, G., Wolfe, A., & Socher, S. H. (1987). Tumors secreting human TNF/cachectin induce cachexia in mice. *Cell*, *50*(4), 555–563. https://doi.org/10.1016/0092-8674(87)90028-6

Park, S. Y., Hwang, B. O., & Song, N. Y. (2023). The role of myokines in cancer: crosstalk between skeletal muscle and tumor. *BMB Reports*, *56*(7), 365–373. https://doi.org/10.5483/BMBREP.2023-0064

Patel, H. J., & Patel, B. M. (2017). TNF-α and cancer cachexia: Molecular insights and clinical implications. *Life Sciences*, *170*, 56–63. https://doi.org/10.1016/J.LFS.2016.11.033

Paval, D. R., Patton, R., McDonald, J., Skipworth, R. J. E., Gallagher, I. J., & Laird, B. J. (2022). A systematic review examining the relationship between cytokines and cachexia in incurable cancer. *Journal of Cachexia, Sarcopenia and Muscle*, *13*(2), 824–838. https://doi.org/10.1002/JCSM.12912

Penna, F., Costamagna, D., Pin, F., Camperi, A., Fanzani, A., Chiarpotto, E. M., Cavallini, G., Bonelli, G., Baccino, F. M., & Costelli, P. (2013). Autophagic Degradation Contributes to Muscle Wasting in Cancer Cachexia. *The American Journal of Pathology*, *182*(4), 1367–1378. https://doi.org/10.1016/J.AJPATH.2012.12.023

Peris-Moreno, D., Taillandier, D., & Polge, C. (2020). MuRF1/TRIM63, Master Regulator of Muscle Mass. *International Journal of Molecular Sciences 2020, Vol. 21, Page 6663*, *21*(18), 6663. https://doi.org/10.3390/IJMS21186663

Petruzzelli, M., & Wagner, E. F. (2016). Mechanisms of metabolic dysfunction in cancer-associated cachexia. *Genes & Development*, *30*(5), 489–501. https://doi.org/10.1101/GAD.276733.115

Pototschnig, I., Feiler, U., Diwoky, C., Vesely, P. W., Rauchenwald, T., Paar, M., Bakiri, L., Pajed, L., Hofer, P., Kashofer, K., Sukhbaatar, N., Schoiswohl, G., Weichhart, T., Hoefler, G., Bock, C., Pichler, M., Wagner, E. F., Zechner, R., & Schweiger, M. (2023). Interleukin-6 initiates muscle- and adipose tissue wasting in a novel C57BL/6 model of cancer-associated cachexia. *Journal of Cachexia, Sarcopenia and Muscle*, *14*(1), 93. https://doi.org/10.1002/JCSM.13109

Raun, S. H., Ali, M. S., Han, X., Henríquez-Olguín, C., Pham, T. C. P., Knudsen, J. R., Willemsen, A. C. H., Larsen, S., Jensen, T. E., Langen, R., & Sylow, L. (2022). AMPK is elevated in human cachectic muscle and prevents cancer-induced metabolic dysfunction in mice. *BioRxiv*, 2022.06.07.495096. https://doi.org/10.1101/2022.06.07.495096

Raun, S. H., Knudsen, J. R., Han, X., Jensen, T. E., & Sylow, L. (2022). Cancer causes dysfunctional insulin signaling and glucose transport in a muscle-type-specific manner. *The FASEB Journal*, *36*(3), e22211. https://doi.org/10.1096/FJ.202101759R

Reed, S. A., Sandesara, P. B., Senf, S. M., & Judge, A. R. (2012). Inhibition of FoxO transcriptional activity prevents muscle fiber atrophy during cachexia and induces hypertrophy. *The FASEB Journal*, *26*(3), 987. https://doi.org/10.1096/FJ.11-189977

Rohm, M., & Herzig, S. (2020). An Antibody Attack against Body Wasting in Cancer. In *Cell Metabolism* (Vol. 32, Issue 3, pp. 331–333). Cell Press. https://doi.org/10.1016/j.cmet.2020.08.003

Rohm, M., Zeigerer, A., Machado, J., & Herzig, S. (2019). Energy metabolism in cachexia. *EMBO Reports*, *20*(4), 1–13. https://doi.org/10.15252/embr.201847258

Romanello, V., & Sandri, M. (2010). Mitochondrial biogenesis and fragmentation as regulators of muscle protein degradation. *Current Hypertension Reports*, *12*(6), 433–439. https://doi.org/10.1007/s11906-010-0157-8

Sacheck, J. M., Hyatt, J.-P. K., Raffaello, A., Jagoe, R. T., Roy, R. R., Edgerton, V. R., Lecker, S. H., & Goldberg, A. L. (2007). Rapid disuse and denervation atrophy involve transcriptional changes similar to those of muscle wasting during systemic diseases. *FASEB Journal : Official Publication of the Federation of American Societies for Experimental Biology*, *21*(1), 140–155. https://doi.org/10.1096/fj.06-6604com

Sanchez, A. M. J., Bernardi, H., Py, G., & Candau, R. B. (2014). Autophagy is essential to support skeletal muscle plasticity in response to endurance exercise. *American Journal of Physiology - Regulatory Integrative and Comparative Physiology*, *307*(8), R956–R969. https://doi.org/10.1152/AJPREGU.00187.2014/ASSET/IMAGES/LARGE/ZH60201485740003.JPEG

Sandri, M. (2008). Signaling in muscle atrophy and hypertrophy. *Physiology*, *23*(3), 160–170. https://doi.org/10.1152/physiol.00041.2007

Sandri, M. (2013). Protein breakdown in muscle wasting: Role of autophagy-lysosome and ubiquitin-proteasome. *International Journal of Biochemistry and Cell Biology*, *45*(10), 2121–2129. https://doi.org/10.1016/j.biocel.2013.04.023

Sandri, M., Sandri, C., Gilbert, A., Skurk, C., Calabria, E., Picard, A., Walsh, K., Schiaffino, S., Lecker, S. H., & Goldberg, A. L. (2004). Foxo Transcription Factors Induce the Atrophy-Related

Ubiquitin Ligase Atrogin-1 and Cause Skeletal Muscle Atrophy. *Cell*, *117*(3), 399–412. https://doi.org/10.1016/S0092-8674(04)00400-3

Sartori, R., Gregorevic, P., & Sandri, M. (2014). TGFβ and BMP signaling in skeletal muscle: Potential significance for muscle-related disease. *Trends in Endocrinology and Metabolism*, *25*(9), 464–471. https://doi.org/10.1016/j.tem.2014.06.002

Sartori, R., Hagg, A., Zampieri, S., Armani, A., Winbanks, C. E., Viana, L. R., Haidar, M., Watt, K. I., Qian, H., Pezzini, C., Zanganeh, P., Turner, B. J., Larsson, A., Zanchettin, G., Pierobon, E. S., Moletta, L., Valmasoni, M., Ponzoni, A., Attar, S., … Sandri, M. (2021). Perturbed BMP signaling and denervation promote muscle wasting in cancer cachexia. *Science Translational Medicine*, *13*(605). https://doi.org/10.1126/SCITRANSLMED.AAY9592

Sartori, R., Milan, G., Patron, M., Mammucari, C., Blaauw, B., Abraham, R., & Sandri, M. (2009). Smad2 and 3 transcription factors control muscle mass in adulthood. *American Journal of Physiology - Cell Physiology*, *296*(6), 1248–1257. https://doi.org/10.1152/AJPCELL.00104.2009/SUPPL_FILE/SUPPLEMENTAL

Sartori, R., Romanello, V., & Sandri, M. (2021a). Mechanisms of muscle atrophy and hypertrophy: implications in health and disease. *Nature Communications*, *12*(1), 1–12. https://doi.org/10.1038/s41467-020-20123-1

Sartori, R., Schirwis, E., Blaauw, B., Bortolanza, S., Zhao, J., Enzo, E., Stantzou, A., Mouisel, E., Toniolo, L., Ferry, A., Stricker, S., Goldberg, A. L., Dupont, S., Piccolo, S., Amthor, H., & Sandri, M. (2013). BMP signaling controls muscle mass. *Nature Genetics 2013 45:11*, *45*(11), 1309–1318. https://doi.org/10.1038/ng.2772

Schmidt, S. F., Rohm, M., Herzig, S., & Berriel Diaz, M. (2018a). Cancer Cachexia: More Than Skeletal Muscle Wasting. *Trends in Cancer*, *4*(12), 849–860. https://doi.org/10.1016/j.trecan.2018.10.001

Schmidt, S. F., Rohm, M., Herzig, S., & Berriel Diaz, M. (2018b). Cancer Cachexia: More Than Skeletal Muscle Wasting. *Trends in Cancer*, *4*(12), 849–860. https://doi.org/10.1016/j.trecan.2018.10.001

Scicchitano, B. M., Dobrowolny, G., Sica, G., & Musarò, A. (2018). Molecular Insights into Muscle Homeostasis, Atrophy and Wasting. *Current Genomics*, *19*(5), 356. https://doi.org/10.2174/1389202919666180101153911

Setiawan, T., Sari, I. N., Wijaya, Y. T., Julianto, N. M., Muhammad, J. A., Lee, H., Chae, J. H., & Kwon, H. Y. (2023). Cancer cachexia: molecular mechanisms and treatment strategies. *Journal of Hematology & Oncology*, *16*(1), 54. https://doi.org/10.1186/S13045-023-01454-0

Space Ranger - Official 10x Genomics Support. (n.d.). Retrieved February 6, 2024, from https://www.10xgenomics.com/support/software/space-ranger/latest

Sukari, A., Muqbil, I., Mohammad, R. M., Philip, P. A., & Azmi, A. S. (2016). F-BOX proteins in cancer cachexia and muscle wasting: emerging regulators and therapeutic opportunities. *Seminars in Cancer Biology*, *36*, 95. https://doi.org/10.1016/J.SEMCANCER.2016.01.002

Suriben, R., Chen, M., Higbee, J., Oeffinger, J., Ventura, R., Li, B., Mondal, K., Gao, Z., Ayupova, D., Taskar, P., Li, D., Starck, S. R., Chen, H. I. H., McEntee, M., Katewa, S. D., Phung, V., Wang, M., Kekatpure, A., Lakshminarasimhan, D., … Allan, B. B. (2020). Antibody-mediated inhibition of GDF15–GFRAL activity reverses cancer cachexia in mice. *Nature Medicine 2020 26:8*, *26*(8), 1264–1270. https://doi.org/10.1038/s41591-020-0945-x

Sweeney, H. L., & Hammers, D. W. (2018). Muscle contraction. *Cold Spring Harbor Perspectives in Biology*. https://doi.org/https://doi.org/10.1101/cshperspect.a023200

Tajrishi, M. M., Zheng, T. S., Burkly, L. C., & Kumar, A. (2014). The TWEAK-Fn14 pathway: A potent regulator of skeletal muscle biology in health and disease. *Cytokine & Growth Factor Reviews*, *25*(2), 215–225. https://doi.org/10.1016/J.CYTOGFR.2013.12.004

Talbert, E. E., & Guttridge, D. C. (2016). Impaired regeneration: A role for the muscle microenvironment in cancer cachexia. *Seminars in Cell & Developmental Biology*, *54*, 82–91. https://doi.org/10.1016/J.SEMCDB.2015.09.009

Thoma, A., & Lightfoot, A. P. (2018). Nf-kb and inflammatory cytokine signalling: Role in skeletal muscle atrophy. *Advances in Experimental Medicine and Biology*, *1088*, 267–279. https://doi.org/10.1007/978-981-13-1435-3_12/COVER

Tisdale, M. J. (2009). Mechanisms of cancer cachexia. *Physiological Reviews*, *89*(2), 381–410. https://doi.org/10.1152/PHYSREV.00016.2008/ASSET/IMAGES/LARGE/Z9J0020925040009. JPEG

Tsai, V. W. W., Husaini, Y., Sainsbury, A., Brown, D. A., & Breit, S. N. (2018). The MIC-1/GDF15-GFRAL Pathway in Energy Homeostasis: Implications for Obesity, Cachexia, and Other Associated Diseases. In *Cell Metabolism* (Vol. 28, Issue 3, pp. 353–368). Cell Press. https://doi.org/10.1016/j.cmet.2018.07.018

Tsai, V. W. W., Macia, L., Johnen, H., Kuffner, T., Manadhar, R., Jørgensen, S. B., Lee-Ng, K. K. M., Zhang, H. P., Wu, L., Marquis, C. P., Jiang, L., Husaini, Y., Lin, S., Herzog, H., Brown, D. A., Sainsbury, A., & Breit, S. N. (2013). TGF-b Superfamily Cytokine MIC-1/GDF15 Is a Physiological Appetite and Body Weight Regulator. *PLoS ONE*, *8*(2). https://doi.org/10.1371/journal.pone.0055174

Vainshtein, A., & Sandri, M. (2020). Signaling pathways that control muscle mass. *International Journal of Molecular Sciences*, *21*(13), 1–32. https://doi.org/10.3390/ijms21134759

Vegiopoulos, A., Rohm, M., & Herzig, S. (2017). Adipose tissue: between the extremes. *The EMBO Journal*, *36*(14), 1999–2017. https://doi.org/10.15252/embj.201696206

Waddell, D. S., Baehr, L. M., Van Den Brandt, J., Johnsen, S. A., Reichardt, H. M., Furlow, J. D., & Bodine, S. C. (2008). The glucocorticoid receptor and FOXO1 synergistically activate the skeletal muscle atrophy-associated MuRF1 gene. *American Journal of Physiology - Endocrinology and Metabolism*, *295*(4), 785–797. https://doi.org/10.1152/AJPENDO.00646.2007/ASSET/IMAGES/LARGE/ZH10100854250007.JPEG

Walker, B. L., Cang, Z., Ren, H., Bourgain-Chang, E., & Nie, Q. (2022). Deciphering tissue structure and function using spatial transcriptomics. *Communications Biology 2022 5:1*, *5*(1), 1–10. https://doi.org/10.1038/s42003-022-03175-5

Webster, J. M., Kempen, L. J. A. P., Hardy, R. S., & Langen, R. C. J. (2020). Inflammation and Skeletal Muscle Wasting During Cachexia. In *Frontiers in Physiology* (Vol. 11). Frontiers Media S.A. https://doi.org/10.3389/fphys.2020.597675

Wilburn, D., Ismaeel, A., Machek, S., Fletcher, E., & Koutakis, P. (2021). Shared and distinct mechanisms of skeletal muscle atrophy: A narrative review. *Ageing Research Reviews*, *71*, 101463. https://doi.org/10.1016/J.ARR.2021.101463

Winbanks, C. E., Murphy, K. T., Bernardo, B. C., Qian, H., Liu, Y., Sepulveda, P. V., Beyer, C., Hagg, A., Thomson, R. E., Chen, J. L., Walton, K. L., Loveland, K. L., McMullen, J. R., Rodgers, B. D., Harrison, C. A., Lynch, G. S., & Gregorevic, P. (2016). Smad7 gene delivery prevents muscle wasting associated with cancer cachexia in mice. *Science Translational Medicine*, *8*(348). https://doi.org/10.1126/SCITRANSLMED.AAC4976/SUPPL_FILE/8-348RA98_SM.PDF

Winbanks, C. E., Wang, B., Beyer, C., Koh, P., White, L., Kantharidis, P., & Gregorevic, P. (2011). TGF-beta regulates miR-206 and miR-29 to control myogenic differentiation through regulation of HDAC4. *The Journal of Biological Chemistry*, *286*(16), 13805–13814. https://doi.org/10.1074/JBC.M110.192625

Yoon, M. S. (2017). mTOR as a key regulator in maintaining skeletal muscle mass. *Frontiers in Physiology*, *8*(OCT), 294538. https://doi.org/10.3389/FPHYS.2017.00788/BIBTEX

Yoshida, T., & Delafontaine, P. (2020). Mechanisms of IGF-1-Mediated Regulation of Skeletal Muscle Hypertrophy and Atrophy. *Cells*, *9*(9). https://doi.org/10.3390/CELLS9091970

Zhao, J., Brault, J. J., Schild, A., Cao, P., Sandri, M., Schiaffino, S., Lecker, S. H., & Goldberg, A. L. (2007). FoxO3 Coordinately Activates Protein Degradation by the Autophagic/Lysosomal and Proteasomal Pathways in Atrophying Muscle Cells. *Cell Metabolism*, *6*(6), 472–483. https://doi.org/10.1016/J.CMET.2007.11.004

Zhou, R., Yang, G., Zhang, Y., & Wang, Y. (2023). Spatial transcriptomics in development and disease. *Molecular Biomedicine*, *4*(1), 32. https://doi.org/10.1186/S43556-023-00144-0

Zhou, X., Wang, J. L., Lu, J., Song, Y., Kwak, K. S., Jiao, Q., Rosenfeld, R., Chen, Q., Boone, T., Simonet, W. S., Lacey, D. L., Goldberg, A. L., & Han, H. Q. (2010a). Reversal of cancer cachexia and muscle wasting by ActRIIB antagonism leads to prolonged survival. *Cell*, *142*(4), 531–543. https://doi.org/10.1016/j.cell.2010.07.011

Zhu, Y., Zhu, L., Wang, X., & Jin, H. (n.d.). *RNA-based therapeutics: an overview and prospectus*. https://doi.org/10.1038/s41419-022-05075-2

Zimmers, T. A., Davies, M. V., Koniaris, L. G., Haynes, P., Esquela, A. F., Tomkinson, K. N., McPherron, A. C., Wolfman, N. M., & Lee, S. J. (2002). Induction of cachexia in mice by systemically administered myostatin. *Science (New York, N.Y.)*, *296*(5572), 1486–1488. https://doi.org/10.1126/SCIENCE.1069525

Zimmers, T. A., Fishel, M. L., & Bonetto, A. (2016). STAT3 in the Systemic Inflammation of Cancer Cachexia. *Seminars in Cell & Developmental Biology*, *54*, 28. https://doi.org/10.1016/J.SEMCDB.2016.02.009